4-3-2018

Multitarget Joint Delay and Doppler Shift Estimation in Bistatic Passive Radar

Mohammed Rashid
Louisiana State University and Agricultural and Mechanical College, mrashi2@lsu.edu

MULTITARGET JOINT DELAY AND DOPPLER SHIFT ESTIMATION IN BISTATIC PASSIVE RADAR

A Thesis

Submitted to the Graduate Faculty of the
Louisiana State University and
Agricultural and Mechanical College
in partial fulfillment of the
requirements for the degree of
Master of Science in Electrical Engineering

in

School of Electrical Engineering and Computer Science

by
Mohammed Rashid
B.Sc., NWFP University of Engineering & Technology (Pakistan), 2012
May 2018

I dedicate this thesis to my parents, Zahid Mahmood and Zille Huma, and to my best-in-the-world siblings, Rafia Mahmood and Mohammed Sajid.

Acknowledgments

I would like to start by sincerely thanking my adviser Prof. Morteza Naraghi-Pour for his valuable guidance and continuous support during the period of this work. The discussions we had on this work were very helpful to make it possible. His wisdom, professional success, and personal morals encourage me to follow him as a role model in my career and life.

I am also very thankful to my committee members, Prof. Shuangqing Wei and Prof. Xiangwei Zhou, for spending their precious time on reviewing this work and making interesting comments about it.

Finally, I would like to thank my father, Zahid Mahmood, for always praying for me as well as encouraging and guiding me when I was stressed-out and disappointed. Thanks to my beloved mother, Zille Huma, whom exceptional love and prayers have always been a strong source of motivation to me. Also, I am grateful to my siblings, Rafia Mahmood and Mohammed Sajid, for the unbiased love and friendship, they have always shown for me. I specially dedicate this work to all four of you.

Table of Contents

List of Figures

Abstract

Bistatic passive radar (BPR) system does not transmit any electromagnetic signal unlike the active radar, but employs an existing Illuminator of opportunity (IO) in the environment, for instance, a broadcast station, to detect and track the targets of interest. Therefore, a BPR system is comprised of two channels. One is the reference channel that collects only the IO signal, and the other is the surveillance channel which is used to capture the targets' reflected signals. When the IO signal reflected from multiple targets is captured in the surveillance channel (SC) then estimating the delays and Doppler shifts of all the observed targets is a challenging problem. For BPR system, the signal processing algorithms developed so far models the IO waveform as a deterministic process and discretizes the delays and Doppler shifts parameters.

In this thesis, we deal with the problem of jointly estimating the delays and Doppler shifts of multiple targets in a BPR system (i.e., a two channel system) when the unknown IO signal is modeled as a correlated stochastic process. Unlike the previous work, we take all the delays and Doppler shifts as continuous-valued parameters to avoid straddle loss due to discretization and propose a computationally efficient Expectation-Maximization (EM) based algorithm that breaks up the complex multidimensional maximum likelihood optimization problem into multiple separate optimization problems. The EM algorithm jointly provides the estimates of all the delays and Doppler shifts of the targets along with the estimate of each target's component signal in the SC and the estimate of the unknown IO signal. We also derive the Cramer-Rao lower bound for the considered multitarget estimation problem with stochastic IO signal. Numerical simulations are presented where we compare our proposed EM-based multi-target estimator with the widely used conventional cross correlation estimator under different multitarget environments.

Chapter 1
Introduction

Passive radar has emerged as a powerful technology for many military applications, particularly in the air defense systems. A passive radar can localize and track the targets of interest by employing the existing broadcast transmitters in the environment, for instance, cell phone base-stations, frequency modulation (FM) radio, digital audio broadcast (DAB), and digital video broadcast terrestrial (DVB-T) stations [1–3]. In this chapter, we first provide a brief background on passive radar with a review of research studies on single target localization. Then we discuss the multiple target delay and Doppler shift estimation in passive radar followed up by a section on the limitations in the published research studies and our contributions in this area. Finally an outline of the forthcoming chapters along with our notations is provided.

1.1 Background

Passive radar has spurred the interest of many researchers over the past years due to its extensive set of advantages over active radar [4–6]. These includes its low cost, covert operation, and counter-stealth behavior. Since passive radar employs an already available broadcast station in the environment for target localization and tracking, it does not require a co-located transmitter as there is in active radar. This property not only lowers the cost of the system and avoids spectral congestion but also makes covert operation possible. Furthermore, since there is a wide set of possible broadcast transmitters in the environment, for instance, cell phone base-stations, FM radio, DAB stations, and DVB-T stations, passive radar can operate in a wide frequency band which assists in increasing the radar cross-section of stealthy targets making counter-stealth operation possible [1–3], [5].

As the transmitter, also called an Illuminator of Opportunity (IO), employed by passive radar is set up for an entirely different purpose, it is not under its control, i.e., the IO is non-cooperative. Therefore in bistatic configuration (called bistatic passive radar (BPR) system), the radar uses a special directional antenna with its main lobe in the radiation

pattern pointing toward the IO to receive only the IO signal. This is called the reference channel (RC). A separate antenna is used with its main lobe in the radiation pattern directing toward the surveillance area to receive the target reflected signal [1, 4–6]. This is called the surveillance channel (SC). Given the RC and SC observed signals, a standard approach it uses for a target localization is to cross-correlate both signals and locate the peak of the cross-correlation (CC) function over a certain grid of parameters to detect and estimate the target parameters [1, 6]. This is similar to the matched filter (MF) operation used in active radar when the transmitter signal is replaced with the RC signal. However, since the RC signal received by the antenna is usually contaminated by noise in the reference channel, the performance of CC is not as good as the MF. In [7], the performance of CC with noisy RC signal under the presence of only single target is evaluated against the MF and the theoretical bounds on CC's performance compared to MF are derived. Considering the same single target scenario and the noise in RC, some improved passive target localization algorithms are also derived in [8, 9] for BPR system. Another configuration of passive radar that is called multistatic passive radar (MPR) system is used when a direct path to the IO signal is not observable through the RC antenna. So an MPR system employs multiple receivers with only SC antenna to collect the target reflected signal on each of them which are then combined to improve the overall signal to noise ratio of the SC signal. The correlation among the different SC signals due to illumination of target by the same IO assists in the target localization. In [10], generalized likelihood ratio test (GLRT) based detectors for the single target observation in an MPR system are derived and the performance is compared with the generalized coherence detector from [11].

When compared to an active radar, a major obstacle in a target localization by passive radar is that the IO waveform is unknown to the receiver. One way to deal with this uncertainty is to model it as an unknown deterministic process in deriving the localization algorithms. Such modeling approach for the IO signal was used to derive GLRT based detection algorithm for a target localization in BPR systems in [8] and for the MPR systems

in [10]. Another approach to handle the unknown IO signal is to model it as a Gaussian process. In [12], an expectation maximization based estimation algorithm was derived for single target case in BPR system by modeling the unknown IO signal as a correlated circularly symmetric complex Gaussian process, whereas for MPR system, the same single target case and IO modeling criterion was used to derive GLRT based detection algorithm in [13]. Second obstacle in target localization by passive radar is the direct path interference and multipath clutter signal observed in the SC signal for which the target localization procedure is often divided into two steps − first one is the interference removal, and the second one is then target localization. To carry out the second step as in [8, 10], it is assumed that the interference has been removed by using a directional antenna for SC and some adaptive signal processing approaches as described in [14–17].

1.2 Multitarget Delays and Dopplers Estimation

When the main lobe of the SC antenna's radiation pattern is wider or there is an array of antennas connected to SC, then reflected signals from multiple targets is captured in the surveillance channel. In [6,18,19], such SC antenna configuration is used in BPR system to detect multiple targets using the CC estimator, whereas for MPR system the group sparsity based algorithm for multiple target tracking using only Doppler measurements is proposed in [20]. Particularly for our focused BPR system, recently GLRT based multiple targets joint delays and Doppler shifts estimation algorithms are derived in [21–23]. While in [21], the multitarget detection problem is tackled as a binary hypothesis testing (BHT) problem of detecting a single target in the presence of other interfering targets, on the other hand, in [22, 23] it is realized as an M-ary hypothesis testing problem with M being the number of existing targets in the SC. The existing targets in the SC are determined sequentially in [22, 23] through a sequence of binary hypothesis testings where the previously detected targets are canceled from the SC signal to remove the interference for detecting new targets and the running sequence of BHT is stopped when the first null hypothesis is detected.

1.3 Limitations and Contribution

Although, the multi-target delay and Doppler shift estimation problem has been tackled in different ways in the work cited above in section 1.2, there are some limitations in those research studies. Firstly, in the studies in [6, 18, 19, 21–23] the two dimensional delay-Doppler uncertainty space is dicretized into small bins and then detection is performed on each bin in a sequential manner. Such discretization of the parameter space compromises its resolution which may result in a straddle loss and degraded performance of the detector. Secondly, [21–23] models the IO waveform as a deterministic process, whereas another approach to deal with the unknown IO waveform is to model it as a stochastic process in which the samples are taken from an independent and identically distributed Gaussian process as in [24]. Moreover, since in today's communication systems, there is channel coding, modulation, and pulse shaping involved in the IO transmitter, the IO samples inherit a correlation with each other. Thus in [12,13], the authors modeled the IO waveform as a correlated Gaussian process to derive single target detection and estimation algorithms for passive radar, but the multiple target localization algorithm for such modeling of IO waveform is not found in the literature of passive radar.

In this thesis, we consider the problem of jointly estimating the time delays and Doppler shifts of multiple targets in a two channel (RC and SC) BPR system where the IO waveform is modeled as a correlated stochastic process. Hence, the algorithms derived in [21–23, 25] do not fit as the solution to our motivated problem. We consider the case when the RC observation is noisy and the direct path interference from the SC observation has been removed by using a directional antenna and some signal processing techniques as mentioned in [14–16] and the references therein. Moreover, we follow [12, 13] to avoid the straddle loss due to the discretization of delay-Doppler parameter space and propose a multiple target signal model where all the associated delays and Doppler shifts are modeled as continuous-valued parameters. As mentioned previously, we also assume that the IO waveform exhibits some sort of time domain correlation between its samples, and therefore, we also include

the auto-correlation matrix of the samples in solving the estimation problem. An EM algorithm is proposed which breaks up the multi-target complex multidimensional maximum likelihood (ML) optimization problem into multiple simple single target optimization problems. Our proposed EM algorithm provides the estimates of the delays, the Doppler shifts, and the SC amplitude coefficients of all the targets along with the estimate of the unknown IO signal and the estimate of the SC component signal of each target in a BPR configuration. Numerical simulations are also included which compare the performance of our proposed EM-based multi-target estimator with the conventional CC estimator under different multiple target environments. In order to access the performance of both estimators we also derive the Cramer-Rao lower bound (CRLB) for the multiple target estimation problem considered in this thesis.

1.4 Outline and Notations

This thesis is further set up as follows. Chapter 2 discusses the relevant work done before on multitarget localization in BPR system, Chapter 3 formulates the problem and discusses the solving approach. It also derives the computationally efficient EM-based multi-target estimator for simplifying the optimization problem, and the CRLB to access the performance of our proposed estimator. Finally, Chapter 4 discusses the numerical simulations and Chapter 5 concludes the work.

The notations used in the following chapters are as follows. A scalar is represented by a non-boldface lower-case letter (x). Each vector is taken as a column vector and it is denoted by a boldface lower case letter ($\mathbf{x}$). Matrices are denoted by boldface upper case letters ($\mathbf{A}$). Superscripts $(.)^*$, $(.)^T$, and $(.)^H$ denote the conjugate, transpose, and Hermitian transpose operations, respectively. $E[.]$ denotes statistical expectation and $\Re(z)$ represents the real part of a complex quantity z. $\odot$ represents the Hadamard product. $\mathbf{I}_N$ is the identity matrix of size N and $\mathbf{0}_{K\times L}$ is a $K \times L$ zero matrix. $\det\{\mathbf{A}\}$ and $\mathrm{tr}\{\mathbf{A}\}$ denotes the determinant and the trace of the matrix $\mathbf{A}$, respectively. Finally, $\|\mathbf{x}\|$ denotes the Euclidean norm of the vector $\mathbf{x}$.

Chapter 2
Multi-target Localization in Bistatic Passive Radar

Multiple target localization is a challenging problem in passive radar for which the standard approach used is based on estimating the delays and Doppler shifts corresponding to all the observed targets in a surveillance channel. Note that to localize multiple targets, the main beam of the antenna pattern connected to the SC is designed wider enough to capture the IO's reflected signal by multiple targets. In this chapter, we discuss briefly the existing relevant signal processing strategies for localizing multiple targets in our focused BPR system.

2.1 Cross-Correlation Estimator

Cross-Correlation (CC) estimator is widely used for detecting the targets and estimating their parameters in BPR systems. Given the RC and SC signals, it computes a cross-correlation function, also called an ambiguity function, over a certain delay-Doppler domain as follow.

$$\boldsymbol{\chi}(k,l) = \left| \sum_{n=0}^{N-1} y_s(n) y_r^*(n-k) e^{\frac{-j2\pi ln}{N}} \right| = \left| FFT\{y_s(n) y_r^*(n-k)\} \right|, \tag{2.1}$$

where $FFT\{.\}$ is the Fast Fourier Transform operation which provides computational efficiency, $y_r(n)$ and $y_s(n)$ are the sampled RC and SC signals, respectively, and N is the number of samples collected. This mimics the matched filtering operation performed in active radar when the transmitter signal is substituted with the RC signal. It is assumed for (2.1) that the delay is $\tau = kT_s$ and the Doppler shift is $f_d = l/NT_s$ (T_s is the sampling interval), so k and l gives the respective delay-Doppler estimates for the observed targets.

The ambiguity function $\boldsymbol{\chi}(k,l)$ evaluated over a certain delay-Doppler grid is then analyzed to find the peaks representing observed targets through a constant false alarm rate (CFAR) detection that is carried out sequentially on each grid point. To perform the CFAR detection on each grid cell (grid point) under test, the cell-averaging CFAR detector considers some guard cells around it and changes the threshold with the estimate of noise

variance computed from the average of the cell values in the training set.

In [6,18,19], CC was used to localize multiple targets in a bistatic passive radar system. However, like in (2.1), the parameters were discretized and thus the detection was performed on a discrete grid of points.

2.2 GLRT based Multi-target Localization

Recently in [22], the author considered the multiple target localization problem in BPR system in the presence of direct path interference and clutter signals. The M-ary hypothesis testing problem is designed as a sequence of multiple binary hypothesis testing problems. The SC signal $\mathbf{x}$ under the two hypotheses is defined as follow.

$$\begin{cases} H_{m-1}: & \mathbf{x} = \mathbf{T}_{m-1}\mathbf{g}_{m-1} + \mathbf{H}\mathbf{c} + \mathbf{n}, \\ H_m: & \mathbf{x} = \mathbf{s}_m\alpha_m + \mathbf{T}_{m-1}\mathbf{g}_{m-1} + \mathbf{H}\mathbf{c} + \mathbf{n}, \end{cases} \tag{2.2}$$

where $m = 1, \ldots, M$. M is the total number of observed targets. $\mathbf{T}_{m-1} = [\mathbf{s}_1, \ldots, \mathbf{s}_{m-1}]$ contains the $m-1$ targets' reflected signals with $\mathbf{s}_m = \left(\mathbf{y}^{(n_m)} \odot \mathbf{e}^{(f_m)}\right)$. $\mathbf{y}^{(n_m)} = \mathbf{P}^{n_m}\mathbf{y}$ where $\mathbf{y}$ contains the RC signal samples. The $\{i,j\}^{th}$ entry of the permutation matrix is $[\mathbf{P}]_{ij} = 1$ if $i = j+1$ and 0 otherwise $\forall\ i,j \in \{0, \ldots, N-1\}$. The n^{th} entry of the vector $[\mathbf{e}^{(f_m)}]_n = e^{j2\pi f_m n T_s}$ for $n = \{0, \ldots, N-1\}$ with T_s being the sampling interval. Furthermore, $\mathbf{g}_{m-1} = [\alpha_1, \ldots, \alpha_{m-1}]^T$ contains the complex amplitudes of $m-1$ targets' reflected signals and the coordinates (n_m, f_m) represent the delay and Doppler shift for the m^{th} target. $\mathbf{H} = [\mathbf{h}_1, \ldots, \mathbf{h}_p, \ldots, \mathbf{h}_P]$ is an $N \times P$ clutter signature matrix with $\mathbf{h}_p = \left(\mathbf{y}^{(n_c^{(p)})} \odot \mathbf{e}^{(f_c^{(p)})}\right)$ and $\left(n_c^{(p)}, f_c^{(p)}\right)$ represents the delay-Doppler coordinates of the p^{th} clutter signature. Finally, $\mathbf{c} = [c_1, \ldots, c_P]^T$ contains the unknown amplitudes of all P clutter signatures and $\mathbf{n}$ represents the noise in the SC which is modeled as circularly symmetrical and complex Gaussian distributed with zero mean and covariance matrix $\sigma^2\mathbf{I}_N$ ($\mathbf{I}_N$ is an identity matrix of size N).

The IO waveform is modeled as deterministic unknown quantity for deriving GLRT, and in (2.2) the RC signal $\mathbf{y}$ is directly taken as the estimate for the IO signal. The unknown

parameter set under the two hypotheses H_{m-1} and H_m is taken as $\boldsymbol{\Theta}_{m-1} = \left\{\mathbf{g}_{m-1}, \mathbf{c}, \sigma^2\right\}$ and $\boldsymbol{\Theta}_m = \left\{(n_m, f_m), \alpha_m, \mathbf{g}_{m-1}, \mathbf{c}, \sigma^2\right\}$. Except (n_m, f_m), all other unknown parameters are replaced with their maximum likelihood estimates under the two hypotheses to obtain the following test statistic for GLRT,

$$\lambda_m(\mathbf{x}) = \frac{2N \left|\mathbf{s}(n_m, f_m)^H \boldsymbol{\Pi}^{\perp}_{\mathbf{U}_{(P+m-1)}} \mathbf{x}\right|^2}{\left|\left|\boldsymbol{\Pi}^{\perp}_{\mathbf{U}_{(P+m-1)}} \mathbf{s}(n_m, f_m)\right|\right|^2 \left|\left|\boldsymbol{\Pi}^{\perp}_{\mathbf{U}_{(P+m-1)}} \mathbf{x}\right|\right|^2}, \tag{2.3}$$

where $\boldsymbol{\Pi}^{\perp}_{\mathbf{U}_{(P+m-1)}} = \mathbf{I} - \mathbf{U}_{(P+m-1)} \left(\mathbf{U}^H_{(P+m-1)} \mathbf{U}_{(P+m-1)}\right)^{-1} \mathbf{U}^H_{(P+m-1)}$ and the interference matrix is $\mathbf{U}_{(P+m-1)} = [\mathbf{H}, \mathbf{T}_{m-1}]$ with $\mathbf{U}_{(P)} = \mathbf{H}$. The previously detected targets and clutter is removed from $\mathbf{x}$ in (2.3) to detect the m^{th} target. Starting from $m = 1$, the new m^{th} target is detected if the peak value of $\lambda_m(\mathbf{x})$ exceeds the threshold at the delay-Doppler coordinates (n_m, f_m) which then gives the maximum likelihood estimates of delay and Doppler shift for the target. The sequence of above binary hypothesis tests is repeated until the occurrence of first rejection.

Simulation results were included to show the effectiveness of the proposed detection algorithm in FM and DVB-T based BPR systems. The performance of such GLRT based algorithm is also evaluated in [23] with the analog terrestrial TV signal and computationally efficient implementation is derived. The limitation of the work in [22, 23] is that the delays and Doppler shifts are discretized which may lead to straddle performance loss, and also the IO waveform is treated as a deterministic unknown process in the algorithm. Another approach is to model it as stochastic process where the samples are taken from a correlated Gaussian process as used in [12, 13] for the BPR system. However, [12, 13] only considered the single target scenario and the localization algorithm for the multiple targets observation case with such modeling of the IO signal is not found in the literature of BPR system.

Chapter 3
Problem Formulation and EM based Solution

Considering the limitations of the relevant work discussed before, this chapter first formulates a system model to jointly estimate the delays and Doppler shifts of observed multiple targets in a bistatic passive radar system. There we treat all the delays and Doppler shifts as continuous-valued parameters in order to avoid the straddle performance loss due to their discretization, and model the IO waveform as a correlated stochastic process. Next discussing the problem at hand and the solving approach, an EM-based computationally efficient estimator is derived. CRLB is also derived in this chapter to access the performance of our proposed estimator.

3.1 System Model

We consider the BPR system shown in Fig. 3.1 which is comprised of a non-cooperative IO and a passive radar with two channels, i.e., RC and SC. The RC is assumed to be using a directional antenna facing toward the IO to only obtain the unknown source signal and the SC is supposed to be using an another directional antenna with its main lobe covering the surveillance area to receive the targets' reflected signals. We suppose that the direct path interference in the SC has been removed by using digital beamforming and filtering methods as discussed in [10, 14–16]. Thus the signals received in the RC and SC can be written as

$$y_r^{'}(t) = \gamma x^{'}(t - t_r) + u^{'}(t), \tag{3.1}$$

$$y_s^{'}(t) = \sum_{m=1}^{M} \alpha_m^{'} x^{'}(t - t_m^s) e^{j2\pi f_m^d t} + v^{'}(t), \tag{3.2}$$

where $x^{'}(t)$ is the unknown baseband signal of IO, γ is the amplitude coefficient for the channel propagation effects from IO to RC, t_r is the propagation delay in that path, and $u^{'}(t)$ is the zero mean Gaussian disturbance that models clutter and the receiver noise in RC. M is the total number of targets observed by the SC, $\alpha_m^{'}$ is the amplitude coefficient

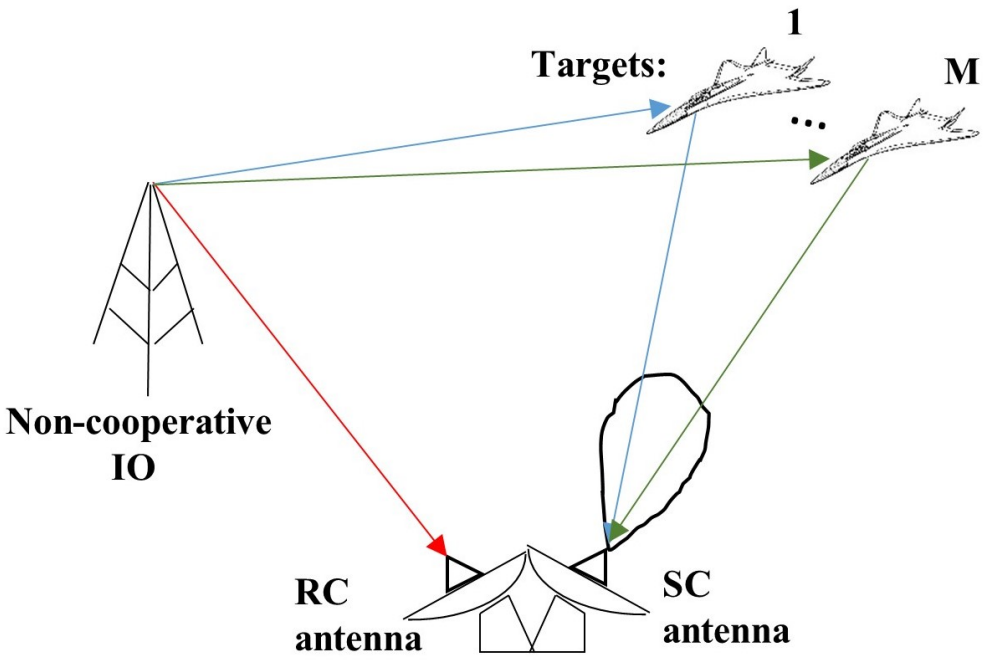

Figure 3.1: Configuration of Bistatic Passive Radar System

for the channel propagation effects from IO-to-m^{th} target and from m^{th} target-to-SC and t_m^s is the propagation delay in that path. f_m^d is the m^{th} target Doppler shift and $v^{'}(t)$ is the zero mean Gaussian disturbance that models any residual DPI, clutter, and the receiver noise in SC. We assume that the number of targets M has been determined using some model-order selection method (e.g., see [26, 27]).

Since the location of the IO is usually available which means t_r is known to us. Thus, we can compensate t_r in the RC and SC signals in (3.1) and (3.2) by defining $y_r(t) = y_r^{'}(t+t_r)$ and $y_s(t) = y_s^{'}(t+t_r)$. The noise signals $u(t)$ and $v(t)$ are similarly compensated for t_r. Further, since both γ and $x^{'}(t)$ are unknown so for simplification we subsume them into each other by defining $x(t) = \gamma x^{'}(t)$. Thus, our RC and SC signal models in (3.1) and (3.2)

simplifies as such

$$y_r(t) = x(t) + u(t), \tag{3.3}$$

$$y_s(t) = \sum_{m=1}^{M} \alpha_m x(t - \tau_m) e^{j2\pi f_m^d t} + v(t), \tag{3.4}$$

where $\alpha_m = \alpha_m^{'} e^{j2\pi f_m^d t_r}/\gamma$ and $\tau_m = t_m^s - t_r$ is called the bistatic delay for the m^{th} target in passive radar. Now usually the IO transmits its signal in a frame-by-frame manner where each frame is of a particular duration T. Therefore, we can assume that $x(t)$ is of duration T seconds with a bandwidth of B Hertz. Also, we let that τ^* and f^* are the maximum Bistatic delay and Doppler shift of interest in the BPR configuration. The passive radar receiver observes the RC and SC signals over the observation window of duration T_0 seconds with $T_0 \geq T + \tau^*$ and collects N samples of them with sampling frequency $f_s \geq 2(B + f^*)$ over the time period T_0, where $T_0 = NT_s$ and $T_s = 1/f_s$. Then for $\overline{\mathbf{x}}(\tau_m) = [x(0 - \tau_m), x(T_s - \tau_m), \ldots, x((N-1)T_s - \tau_m)]^T$, $\overline{\mathbf{a}}(f_m^d) = [1, e^{j2\pi f_m^d T_s}, \ldots, e^{j2\pi f_m^d (N-1)T_s}]^T$, and with vectors $\overline{\mathbf{y}}_r$, $\overline{\mathbf{y}}_s$, $\overline{\mathbf{x}}$, $\overline{\mathbf{u}}$ and $\overline{\mathbf{v}}$ similarly defined, we can write the vectorized form of our signal model in discrete-time as

$$\overline{\mathbf{y}}_r = \overline{\mathbf{x}} + \overline{\mathbf{u}}, \tag{3.5}$$

$$\overline{\mathbf{y}}_s = \sum_{m=1}^{M} \alpha_m \overline{\mathbf{x}}(\tau_m) \odot \overline{\mathbf{a}}(f_m^d) + \overline{\mathbf{v}}, \tag{3.6}$$

Herein, we consider that $\overline{\mathbf{x}}$, $\overline{\mathbf{u}}$, and $\overline{\mathbf{v}}$ are all independent of each other and that each one has a zero mean Gaussian distribution with covariance matrices $\mathbf{R}_x$, $\mathbf{R}_u$ and $\mathbf{R}_v$, respectively. In particular, the assumption about the distribution of $\overline{\mathbf{x}}$ is justified for the IO that uses a multiple subcarrier transmission technique, for instance, Orthogonal Frequency Division Multiplexing (OFDM) [28]. For large number of sub-carriers their signal can be approximated by a Gaussian distribution according to the Central Limit Theorem (CLT) [29]. In practice, $\mathbf{R}_x$, $\mathbf{R}_u$, and $\mathbf{R}_v$ could be unknown then they can be

replaced by the sample covariance matrices estimated from the training data [30], but here we take them as known to us.

Next we take $\overline{\mathbf{y}}_r$ and $\overline{\mathbf{y}}_s$ into the frequency domain, and therefore, to take the Discrete Fourier Transform (DFT) of above equations (3.5) and (3.6), we define the N-DFT matrix $\mathbf{F}$ with the $\{k,l\}^{th}$ entry as $[\mathbf{F}]_{k,l} = \frac{1}{\sqrt{N}} e^{-j2\pi(k-1)\Delta f(l-1)T_s}$, $\forall\ k,l \in \{1,2,\ldots,N\}$ and the frequency resolution as $\Delta f = \frac{fs}{N}$. We multiply it on both sides of (3.5) and (3.6) and use the DFT properties [31] to get,

$$\mathbf{y}_r = \mathbf{x} + \mathbf{u}, \tag{3.7}$$

$$\mathbf{y}_s = \sum_{m=1}^{M} \alpha_m \mathbf{A}\left(f_m^d\right) \mathbf{W}\left(\tau_m\right) \mathbf{x} + \mathbf{v}, \tag{3.8}$$

where $\mathbf{y}_r = \mathbf{F}\overline{\mathbf{y}}_r$, $\mathbf{y}_s = \mathbf{F}\overline{\mathbf{y}}_s$, and $\mathbf{x}$, $\mathbf{u}$, and $\mathbf{v}$ are similarly defined. Each vector $\mathbf{x}$, $\mathbf{u}$, and $\mathbf{v}$ still have Gaussian distribution with zero mean, but with the new covariance matrices $\mathbf{\Sigma}_x = \mathbf{F}\mathbf{R}_x\mathbf{F}^H$, $\mathbf{\Sigma}_u = \mathbf{F}\mathbf{R}_u\mathbf{F}^H$, and $\mathbf{\Sigma}_v = \mathbf{F}\mathbf{R}_v\mathbf{F}^H$, respectively. Further in (3.8), $\mathbf{W}\left(\tau_m\right)$ is a diagonal matrix with the k^{th} entry as $\left[\mathbf{W}\left(\tau_m\right)\right]_{k,k} = e^{-j2\pi(k-1)\Delta f\tau_m}$, $\forall\ k \in \{1,2,\ldots,N\}$ and $\mathbf{A}\left(f_m^d\right)$ is a circulant matrix formed by the vector $\mathbf{a}(f_m^d) = \mathbf{F}\overline{\mathbf{a}}(f_m^d)$. The (k,l) entry of the matrix $\mathbf{A}(f_m^d)$ is given by

$$[\mathbf{A}(f_m^d)]_{k,l} = \frac{1}{\sqrt{N}} a_m((k-l)\Delta f), \tag{3.9}$$

$\forall\ k,l \in \{1,2,\ldots,N\}$ and because $\{a_m(n\Delta f)\}$ is a periodic sequence with period N, we have $a_m(-n\Delta f) = a_m((N-n)\Delta f)$ where $a_m(n\Delta f)$ is given by

$$a_m(n\Delta f) = \begin{cases} \sqrt{N} & \forall\ n = \frac{f_m^d}{\Delta f} \\ \dfrac{1-e^{j2\pi\left(\frac{f_m^d}{\Delta f}-n\right)}}{\sqrt{N}\left[1-e^{j\frac{2\pi}{N}\left(\frac{f_m^d}{\Delta f}-n\right)}\right]} & \text{otherwise,} \end{cases} \tag{3.10}$$

$\forall\ n \in \{0,1,\ldots,(N-1)\}$.

3.2 Problem Statement and Solving approach

Now consider that $\mathbf{y} = [\mathbf{y}_r^T, \mathbf{y}_s^T]_{1\times 2N}^T$, then $\mathbf{y}$ is a circularly symmetrical and complex Gaussian random vector with zero mean and covariance matrix $\mathbf{\Sigma}_y(\mathbf{\Theta})$:

$$\mathbf{\Sigma}_y(\mathbf{\Theta}) = \mathrm{E}[\mathbf{y}\mathbf{y}^H] = \begin{bmatrix} \mathbf{D} & \mathbf{P}(\mathbf{\Theta}) \\ \mathbf{P}^H(\mathbf{\Theta}) & \mathbf{B}(\mathbf{\Theta}) \end{bmatrix}_{2N\times 2N}, \tag{3.11}$$

with each block matrix as

$$\mathbf{D} = \mathbf{\Sigma}_x + \mathbf{\Sigma}_u, \tag{3.12}$$

$$\mathbf{P}(\mathbf{\Theta}) = \mathbf{\Sigma}_x \left(\sum_{m=1}^{M} \alpha_m \mathbf{A}(f_m^d)\mathbf{W}(\tau_m) \right)^H, \tag{3.13}$$

$$\mathbf{B}(\mathbf{\Theta}) = \left(\sum_{m=1}^{M} \alpha_m \mathbf{A}(f_m^d)\mathbf{W}(\tau_m) \right) \mathbf{\Sigma}_x \left(\sum_{m=1}^{M} \alpha_m \mathbf{A}(f_m^d)\mathbf{W}(\tau_m) \right)^H + \mathbf{\Sigma}_v, \tag{3.14}$$

So given $\mathbf{y}$ with $\boldsymbol{\theta}_m \triangleq [\alpha_m, \tau_m, f_m^d]^T$ and $\mathbf{\Theta} \triangleq [\boldsymbol{\theta}_1^T, \boldsymbol{\theta}_2^T, \ldots, \boldsymbol{\theta}_M^T]_{1\times 3M}$, the problem at hand is to estimate $\mathbf{\Theta}$. The proposed way is to find the Maximum Likelihood (ML) estimate of $\mathbf{\Theta}$ which is given by

$$\mathbf{\Theta}_{ML} = \arg\min_{\mathbf{\Theta}} \mathbf{S}(\mathbf{\Theta}), \tag{3.15}$$

where

$$\mathbf{S}(\mathbf{\Theta}) = \left[\ln |\mathbf{\Sigma}_y(\mathbf{\Theta})| + \mathbf{y}^H \mathbf{\Sigma}_y^{-1}(\mathbf{\Theta})\mathbf{y} \right], \tag{3.16}$$

but (3.15) is a complex multi-dimensional optimization problem with highly non-linear ML cost function in (3.16). One can think to use the brute-force search method to roughly locate the global minimum point of $\mathbf{S}(\mathbf{\Theta})$ on a coarse grid and then employ the iterative gradient search algorithms, for instance, Newton method, with that point as the initial estimate. However, these methods when applied to solve (3.15) becomes computationally very difficult because of the multi-dimensionality of parameter space.

3.3 EM-based Multi-target Estimator

In this section, we propose an alternative solution using the EM algorithm that simplifies the complicated multi-dimensional ML optimization problem in (3.15).

To begin, as discussed in [32], the first step for writing the EM-based algorithm is to select the complete data $\mathbf{h}$. To choose that, we decompose $\mathbf{y}_s$ into its signal components and write it as $\mathbf{y}_s = \sum_{m=1}^{M} \mathbf{z}_m$ with the m^{th} component represented by

$$\mathbf{z}_m = \alpha_m \mathbf{A}(f_m^d)\mathbf{W}(\tau_m)\mathbf{x} + \mathbf{v}_m, \tag{3.17}$$

where $\mathbf{v}_m$ is the respective noise component such that $\sum_{m=1}^{M} \mathbf{v}_m = \mathbf{v}$. Further we assume that the $\mathbf{v}_m$s' are all independent of each other, and each one has a circularly symmetric complex Gaussian distribution with zero mean and covariance matrix $\mathbf{\Sigma}_v^m = \beta_m \mathbf{\Sigma}_v$. The β_ms' are arbitrary real valued constants that satisfies $\sum_{m=1}^{M} \beta_m = 1$ with $\beta_m \geq 0$. Thus, for $\mathbf{z}$ defined as $\mathbf{z} = [\mathbf{z}_1^T, \mathbf{z}_2^T, \ldots, \mathbf{z}_M^T]_{1\times MN}^T$, we select the complete data $\mathbf{h}$ for our EM-based algorithm as

$$\mathbf{h} = [\mathbf{z}^T, \mathbf{x}^T]^T, \tag{3.18}$$

The log-likelihood function (LLF) of $\mathbf{h}$ given the parameters $\mathbf{\Theta}$ is shown in (A.1) in Appendix A. The EM algorithm is an iterative algorithm that starts with an initial estimate $\mathbf{\Theta}^0$ and repeatedly performs two steps at each iteration, namely the Expectation step (E-step) and the Maximization step (M-step). At the $(p+1)$ iteration, the E-step evaluates the expectation of the complete data LLF in (A.1) given the observed data vector $\mathbf{y}$ and the estimate of the unknown parameters $\mathbf{\Theta}$ from the pth iteration, namely

$$Q(\mathbf{\Theta}; \mathbf{\Theta}^p) = E[L(\mathbf{\Theta}; \mathbf{h}) \mid \mathbf{y}, \mathbf{\Theta}^p], \tag{3.19}$$

In the M-step, we maximize (3.19) over $\boldsymbol{\Theta}$ to find $\boldsymbol{\Theta}^{(p+1)}$, the new estimate of $\boldsymbol{\Theta}$, i.e.,

$$\boldsymbol{\Theta}^{(p+1)} = \arg\max_{\boldsymbol{\Theta}} Q(\boldsymbol{\Theta}; \boldsymbol{\Theta}^p), \tag{3.20}$$

The iterations are performed repeatedly until some convergence criterion is satisfied.

The E-step in (3.19) is computed in Appendix A. By observing $Q(\boldsymbol{\Theta}; \boldsymbol{\Theta}^p)$ given in (A.2), it can be concluded that (3.20) is equivalent to

$$\boldsymbol{\theta}_m^{p+1} = \arg\max_{\boldsymbol{\theta}_m} Q_1(\boldsymbol{\theta}_m; \boldsymbol{\Theta}^p), \tag{3.21}$$

where $Q_1(\boldsymbol{\theta}_m; \boldsymbol{\Theta}^p)$ is given by

$$\begin{aligned} Q_1(\boldsymbol{\theta}_m; \boldsymbol{\Theta}^p) = 2\Re\left\{\alpha_m \mathrm{tr}\left\{\boldsymbol{\Gamma}_2\left(f_m^d, \tau_m\right)\boldsymbol{\Sigma}_{xz|y}^{m,p}\right\}\right\} \\ - |\alpha_m|^2 \mathrm{tr}\left\{\boldsymbol{\Gamma}_2\left(f_m^d, \tau_m\right)\boldsymbol{\Sigma}_{xx|y}^{p}\boldsymbol{\Gamma}_0^H\left(f_m^d, \tau_m\right)\right\}, \end{aligned} \tag{3.22}$$

where the conditional covariance matrices $\boldsymbol{\Sigma}_{xz|y}^{m,p}$ and $\boldsymbol{\Sigma}_{xx|y}^{p}$ are derived in (A.9) and (A.10), respectively, and $\boldsymbol{\Gamma}_0\left(f_m^d, \tau_m\right) \triangleq \mathbf{A}(f_m^d)\mathbf{W}(\tau_m)$ and $\boldsymbol{\Gamma}_2\left(f_m^d, \tau_m\right) \triangleq \left(\boldsymbol{\Sigma}_v^m\right)^{-1}\boldsymbol{\Gamma}_0\left(f_m^d, \tau_m\right)$ (see Appendix A). In order to further simplify the maximization step in (3.21) using [33] we take partial derivative of (3.22) with respect to α_m^* and obtain the following closed form solution

$$\alpha_m^{p+1} = \frac{\mathrm{tr}\left\{\left(\boldsymbol{\Sigma}_{xz|y}^{m,p}\right)^H \boldsymbol{\Gamma}_2^H\left(f_m^{d,p+1}, \tau_m^{p+1}\right)\right\}}{\mathrm{tr}\left\{\boldsymbol{\Gamma}_2\left(f_m^{d,p+1}, \tau_m^{p+1}\right)\boldsymbol{\Sigma}_{xx|y}^{p}\boldsymbol{\Gamma}_0^H\left(f_m^{d,p+1}, \tau_m^{p+1}\right)\right\}}. \tag{3.23}$$

Next we plug (3.23) into (3.22) to remove the dependence on α_m. Thus, the remaining optimization problem simplifies into the following two-dimensional maximization problem which is solved using the Quasi-Newton method.

$$\left(\tau_m^{(p+1)}, f_m^{d,(p+1)}\right) = \arg\max_{\left(\tau_m, f_m^d\right)} Q_2(\tau_m, f_m^d; \boldsymbol{\Theta}^p), \tag{3.24}$$

where $Q_2(\tau_m, f_m^d; \mathbf{\Theta}^p)$ is given by

$$Q_2(\tau_m, f_m^d; \mathbf{\Theta}^p) = \frac{\left|\text{tr}\left\{\mathbf{\Gamma}_2\left(f_m^d, \tau_m\right)\mathbf{\Sigma}_{xz|y}^{m,p}\right\}\right|^2}{\text{tr}\left\{\mathbf{\Gamma}_2\left(f_m^d, \tau_m\right)\mathbf{\Sigma}_{xx|y}^{p}\mathbf{\Gamma}_0^H\left(f_m^d, \tau_m\right)\right\}}, \tag{3.25}$$

Our proposed algorithm, called the EM-based Multitarget Estimator, is summarized in Algorithm 1.

Data: observed signal vectors $\mathbf{y}_r$ and $\mathbf{y}_s$
Result: estimate of the parameter set $\mathbf{\Theta}$

begin
  Estimating the unknown $\mathbf{\Theta}$ *using EM-Algorithm:*
  Assume an initial estimate $\mathbf{\Theta}^0$, set $p = 0$, and $\beta_m = 1/M$;
  while $||\mathbf{\Theta}^{p+1} - \mathbf{\Theta}^p|| \geq \epsilon$ **do**
    1. Use $\mathbf{\Theta}^p$ to compute $\mathbf{K}_0$ and $\mathbf{K}_1$ using (3.12)-(3.14), (A.7), and (A.8).
    2. Use step 1 to compute $\mathbf{x}^p$ and $\mathbf{\Sigma}_{xx|y}^p$ from (A.5) and (A.9), respectively.
       for *m=1,. . . ,M* **do**
         (a) Compute $\mathbf{z}_m^p$ and $\mathbf{\Sigma}_{xz|y}^{m,p}$ using (A.6) and (A.10), respectively.
         (b) Find τ_m^{p+1} and $f_m^{d,p+1}$ by solving (3.24).
         (c) Using step 2b evaluate (3.23) to get α_m^{p+1}.
       end
    3. set $\mathbf{\Theta}^p = \mathbf{\Theta}^{p+1}$ and $p = p + 1$.
  end
end

Algorithm 1: EM-based Multitarget Estimator

An advantage of our algorithm is that it breaks up the complicated multidimensional maximum likelihood optimization problem in (3.15) into M separate optimization problems and the complexity of the algorithm increases only linearly with M. Moreover, the optimization step of the algorithm can be implemented using M parallel computations. The algorithm also provides an estimate of the unknown IO signal, and an estimate of each target's component signal in SC, where particularly the later one can be used to remove the masking effect of strong targets on the weaker targets by the CC estimator [34].

Remark. In Appendix C, we have shown that given an estimate of α_m from the p^{th} iteration when SC has a colored Gaussian disturbance, then the optimization over (τ_m, f_m^d) using

(3.21) can be approximated as

$$\begin{aligned}&\left(\tau_m^{p+1}, f_m^{d,p+1}\right)\\&\approx \arg\min_{(\tau_m, f_m^d)} || \left(\mathbf{\Sigma}_v^m\right)^{-1/2} \left(\mathbf{z}_m^p - \alpha_m^p \mathbf{A}(f_m^d)\mathbf{W}(\tau_m)\mathbf{x}^p\right)||^2,\end{aligned} \tag{3.26}$$

where $\mathbf{z}_m^p$ represents an estimate of the SC signal component corresponding to the m^{th} target and $\alpha_m^p \mathbf{A}(f_m^d)\mathbf{W}(\tau_m)\mathbf{x}^p$ is the reflected signal from the m^{th} target. So estimating τ_m and f_m^d simplifies to finding a weighted least square solution with $\left(\mathbf{\Sigma}_v^m\right)^{-1/2}$ representing the weighting matrix. Particularly, when the SC has a white Gaussian disturbance with the covariance matrix $\mathbf{\Sigma}_v = \mathbf{I}_N$, then given α_m^p the optimization over (τ_m, f_m^d) using (3.21) is reduced to

$$\begin{aligned}&\left\{\tau_m^{p+1}, f_m^{d,p+1}\right\}\\&\approx \arg\max_{(\tau_m, f_m^d)} \Re\left\{(\mathbf{z}_m^p)^H \alpha_m^p \mathbf{A}(f_m^d)\mathbf{W}(\tau_m)\mathbf{x}^p\right\},\end{aligned} \tag{3.27}$$

We note that in (3.27) the new estimates of τ_m and f_m^d are obtained by obtaining correlation between the two signals $\mathbf{z}_m^p$ and $\alpha_m^p \mathbf{A}(f_m^d)\mathbf{W}(\tau_m)\mathbf{x}^p$ (both signals are described in this remark above) and locating the peak of that function.

3.4 Cramer Rao Lower Bound (CRLB)

In order to access the performance of our algorithm, in the following we derive the CRLB for the system model considered in section 3.1. Let us define the real-valued vector $\mathbf{\Phi} = [\phi_1^{(1)}, \phi_1^{(2)}, \phi_2^{(1)}, \phi_2^{(2)}, \ldots, \phi_M^{(1)}, \phi_M^{(2)}, \tau_1, \ldots, \tau_M, f_1^d, \ldots, f_M^d]^T$ with $\phi_m^{(1)} = \alpha_{R,m}$ and $\phi_m^{(2)} = \alpha_{I,m}$ for $m = 1, \ldots, M$. The scalars $\alpha_{R,m}$ and $\alpha_{I,m}$ represent the real and imaginary parts of α_m, respectively. Then the Fisher Information Matrix (FIM) $\mathbf{J}(\mathbf{\Phi}, \mathbf{y})$ is given by

$$\begin{aligned}\mathbf{J}(\mathbf{\Phi}, \mathbf{y}) &= \mathrm{E}\left[\nabla_{\mathbf{\Phi}} \log p(\mathbf{y} \mid \mathbf{\Phi}) \nabla_{\mathbf{\Phi}}^T \log p(\mathbf{y} \mid \mathbf{\Phi})\right] \\ &= \begin{bmatrix} \mathbf{J}_{1,1} & \mathbf{J}_{1,2} & \ldots & \mathbf{J}_{1,M} & (\mathbf{J}_1^{(\tau)})^T & (\mathbf{J}_1^{(f)})^T \\ \mathbf{J}_{2,1} & \mathbf{J}_{2,2} & \ldots & \mathbf{J}_{2,M} & (\mathbf{J}_2^{(\tau)})^T & (\mathbf{J}_2^{(f)})^T \\ \vdots & \vdots & \ddots & \vdots & \vdots & \vdots \\ \mathbf{J}_{M,1} & \mathbf{J}_{M,2} & \ldots & \mathbf{J}_{M,M} & (\mathbf{J}_M^{(\tau)})^T & (\mathbf{J}_M^{(f)})^T \\ \mathbf{J}_1^{(\tau)} & \mathbf{J}_2^{(\tau)} & \ldots & \mathbf{J}_M^{(\tau)} & \mathbf{J}^{(\tau\tau)} & \mathbf{J}^{(\tau f)} \\ \mathbf{J}_1^{(f)} & \mathbf{J}_2^{(f)} & \ldots & \mathbf{J}_M^{(f)} & \mathbf{J}^{(f\tau)} & \mathbf{J}^{(ff)} \end{bmatrix}, \end{aligned} \tag{3.28}$$

where, by using the Slepian-Bang's formula from [35, p. 525], for $r, s = 1, 2$ and $k, l = 1, \ldots, M$, the elements of each component matrix in (3.28) are given in (3.29) to (3.34) as follows,

$$\begin{aligned}[\mathbf{J}_{k,l}]_{r,s} &= \mathrm{E}\left[\frac{\partial \log p(\mathbf{y} \mid \mathbf{\Phi})}{\partial \phi_k^{(r)}} \frac{\partial^T \log p(\mathbf{y} \mid \mathbf{\Phi})}{\partial \phi_l^{(s)}}\right] \\ &= \mathrm{tr}\left\{\mathbf{\Sigma}_y^{-1}(\mathbf{\Theta}) \frac{\partial \mathbf{\Sigma}_y(\mathbf{\Theta})}{\partial \phi_k^{(r)}} \mathbf{\Sigma}_y^{-1}(\mathbf{\Theta}) \frac{\partial \mathbf{\Sigma}_y(\mathbf{\Theta})}{\partial \phi_l^{(s)}}\right\}, \end{aligned} \tag{3.29}$$

$$\begin{aligned}[\mathbf{J}_l^{(\tau)}]_{k,s} &= \mathrm{E}\left[\frac{\partial \log p(\mathbf{y} \mid \mathbf{\Phi})}{\partial \tau_k} \frac{\partial^T \log p(\mathbf{y} \mid \mathbf{\Phi})}{\partial \phi_l^{(s)}}\right] \\ &= \mathrm{tr}\left\{\mathbf{\Sigma}_y^{-1}(\mathbf{\Theta}) \frac{\partial \mathbf{\Sigma}_y(\mathbf{\Theta})}{\partial \tau_k} \mathbf{\Sigma}_y^{-1}(\mathbf{\Theta}) \frac{\partial \mathbf{\Sigma}_y(\mathbf{\Theta})}{\partial \phi_l^{(s)}}\right\}, \end{aligned} \tag{3.30}$$

$$
\begin{aligned}
[\mathbf{J}_l^{(f)}]_{k,s} &= \mathrm{E}\left[\frac{\partial \log p(\mathbf{y} \mid \mathbf{\Phi})}{\partial f_k^d}\frac{\partial^T \log p(\mathbf{y} \mid \mathbf{\Phi})}{\partial \phi_l^{(s)}}\right] \\
&= \mathrm{tr}\left\{\mathbf{\Sigma}_y^{-1}(\mathbf{\Theta})\frac{\partial \mathbf{\Sigma}_y(\mathbf{\Theta})}{\partial f_k^d}\mathbf{\Sigma}_y^{-1}(\mathbf{\Theta})\frac{\partial \mathbf{\Sigma}_y(\mathbf{\Theta})}{\partial \phi_l^{(s)}}\right\}, \qquad (3.31) \\
[\mathbf{J}^{(\tau\tau)}]_{k,l} &= \mathrm{E}\left[\frac{\partial \log p(\mathbf{y} \mid \mathbf{\Phi})}{\partial \tau_k}\frac{\partial^T \log p(\mathbf{y} \mid \mathbf{\Phi})}{\partial \tau_l}\right] \\
&= \mathrm{tr}\left\{\mathbf{\Sigma}_y^{-1}(\mathbf{\Theta})\frac{\partial \mathbf{\Sigma}_y(\mathbf{\Theta})}{\partial \tau_k}\mathbf{\Sigma}_y^{-1}(\mathbf{\Theta})\frac{\partial \mathbf{\Sigma}_y(\mathbf{\Theta})}{\partial \tau_l}\right\}, \qquad (3.32) \\
[\mathbf{J}^{(f\tau)}]_{k,l} &= \mathrm{E}\left[\frac{\partial \log p(\mathbf{y} \mid \mathbf{\Phi})}{\partial f_k^d}\frac{\partial^T \log p(\mathbf{y} \mid \mathbf{\Phi})}{\partial \tau_l}\right] \\
&= \mathrm{tr}\left\{\mathbf{\Sigma}_y^{-1}(\mathbf{\Theta})\frac{\partial \mathbf{\Sigma}_y(\mathbf{\Theta})}{\partial f_k^d}\mathbf{\Sigma}_y^{-1}(\mathbf{\Theta})\frac{\partial \mathbf{\Sigma}_y(\mathbf{\Theta})}{\partial \tau_l}\right\}, \qquad (3.33) \\
[\mathbf{J}^{(ff)}]_{k,l} &= \mathrm{E}\left[\frac{\partial \log p(\mathbf{y} \mid \mathbf{\Phi})}{\partial f_k^d}\frac{\partial^T \log p(\mathbf{y} \mid \mathbf{\Phi})}{\partial f_l^d}\right] \\
&= \mathrm{tr}\left\{\mathbf{\Sigma}_y^{-1}(\mathbf{\Theta})\frac{\partial \mathbf{\Sigma}_y(\mathbf{\Theta})}{\partial f_k^d}\mathbf{\Sigma}_y^{-1}(\mathbf{\Theta})\frac{\partial \mathbf{\Sigma}_y(\mathbf{\Theta})}{\partial f_l^d}\right\}, \qquad (3.34)
\end{aligned}
$$

and $\mathbf{J}^{(\tau f)} = [\mathbf{J}^{(f\tau)}]^T$. In the above,

$$
\frac{\partial \mathbf{\Sigma}_y(\mathbf{\Theta})}{\partial \phi_k^{(r)}} = \begin{bmatrix} \mathbf{0}_{N\times N} & \mathbf{V}_k^{(r)} \\ \left(\mathbf{V}_k^{(r)}\right)^H & \mathbf{B}_k^{(r)} \end{bmatrix}, \qquad (3.35)
$$

$$
\frac{\partial \mathbf{\Sigma}_y(\mathbf{\Theta})}{\partial \tau_k} = \begin{bmatrix} \mathbf{0}_{N\times N} & \mathbf{V}_k^{(\tau)} \\ \left(\mathbf{V}_k^{(\tau)}\right)^H & \mathbf{B}_k^{(\tau)} \end{bmatrix}, \qquad (3.36)
$$

$$
\frac{\partial \mathbf{\Sigma}_y(\mathbf{\Theta})}{\partial f_k^d} = \begin{bmatrix} \mathbf{0}_{N\times N} & \mathbf{V}_k^{(f)} \\ \left(\mathbf{V}_k^{(f)}\right)^H & \mathbf{B}_k^{(f)} \end{bmatrix}, \qquad (3.37)
$$

where

$$
\mathbf{V}_k^{(1)} = \mathbf{\Sigma}_x \mathbf{\Gamma}_0^H(f_k^d, \tau_k), \qquad (3.38)
$$

$$
\mathbf{V}_k^{(2)} = -j\mathbf{V}_k^{(1)}, \qquad (3.39)
$$

$$
\mathbf{V}_k^{(\tau)} = \alpha_k^* \mathbf{\Sigma}_x \dot{\mathbf{W}}^H(\tau_k)\mathbf{A}^H(f_k^d), \qquad (3.40)
$$

and

$$\mathbf{V}_k^{(f)} = \alpha_k^* \mathbf{\Sigma}_x \mathbf{W}^H(\tau_k) \dot{\mathbf{A}}^H(f_k^d), \tag{3.41}$$

$$\mathbf{B}_k^{(1)} = \mathbf{\Gamma}_0(f_k^d, \tau_k)\mathbf{\Sigma}_x \left(\sum_{m=1}^{M} \mathbf{\Gamma}_1(\boldsymbol{\theta}_m)\right)^H + \mathbf{\Gamma}_0^H(f_k^d, \tau_k)\mathbf{\Sigma}_x \left(\sum_{m=1}^{M} \mathbf{\Gamma}_1(\boldsymbol{\theta}_m)\right), \tag{3.42}$$

$$\mathbf{B}_k^{(2)} = j\mathbf{\Gamma}_0(f_k^d, \tau_k)\mathbf{\Sigma}_x \left(\sum_{m=1}^{M} \mathbf{\Gamma}_1(\boldsymbol{\theta}_m)\right)^H - j\mathbf{\Gamma}_0^H(f_k^d, \tau_k)\mathbf{\Sigma}_x \left(\sum_{m=1}^{M} \mathbf{\Gamma}_1(\boldsymbol{\theta}_m)\right), \tag{3.43}$$

$$\mathbf{B}_k^{(\tau)} = \alpha_k \mathbf{A}(f_k^d)\dot{\mathbf{W}}(\tau_k)\mathbf{\Sigma}_x \left(\sum_{m=1}^{M} \mathbf{\Gamma}_1(\boldsymbol{\theta}_m)\right)^H + \left(\alpha_k \mathbf{A}(f_k^d)\dot{\mathbf{W}}(\tau_k)\right)^H \mathbf{\Sigma}_x \left(\sum_{m=1}^{M} \mathbf{\Gamma}_1(\boldsymbol{\theta}_m)\right), \tag{3.44}$$

$$\mathbf{B}_k^{(f)} = \alpha_k \dot{\mathbf{A}}(f_k^d)\mathbf{W}(\tau_k)\mathbf{\Sigma}_x \left(\sum_{m=1}^{M} \mathbf{\Gamma}_1(\boldsymbol{\theta}_m)\right)^H + \left(\alpha_k \dot{\mathbf{A}}(f_k^d)\mathbf{W}(\tau_k)\right)^H \mathbf{\Sigma}_x \left(\sum_{m=1}^{M} \mathbf{\Gamma}_1(\boldsymbol{\theta}_m)\right), \tag{3.45}$$

Finally, $\mathbf{\Gamma}_1(\boldsymbol{\theta}_m) = \alpha_m \mathbf{\Gamma}_0\left(f_m^d, \tau_m\right)$ (see Appendix A), the k^{th} entry of the diagonal matrix $\dot{\mathbf{W}}$ is given by

$$[\dot{\mathbf{W}}]_{k,k} = -j2\pi\Delta f(k-1)e^{-j2\pi\Delta f(k-1)\tau_m}, \tag{3.46}$$

and the (k,l) entry of $\dot{\mathbf{A}}$ matrix is given by

$$[\dot{\mathbf{A}}\left(f_m^d\right)]_{k,l} = \begin{cases} 0 & \text{if } \left|k - l - \frac{f_m^d}{\Delta f}\right| = 0 \text{ or } N \\ \frac{j2\pi}{N^2\Delta f}\left[1-\gamma_{k,l}^m\right]^{-2} \times & \\ \left[\gamma_{k,l}^m + (N-1)\left(\gamma_{k,l}^m\right)^{N+1} - N\left(\gamma_{k,l}^m\right)^N\right] & \\ & \text{otherwise,} \end{cases} \tag{3.47}$$

where $\gamma_{k,l}^m = e^{j\frac{2\pi}{N}\left(\frac{f_m^d}{\Delta f} - k + l\right)}$ for $k, l = 1, 2, \ldots, N$. Thus the CRLB on $\mathbf{\Phi}(i)$ for $i = 1, \ldots, 4M$ is given by

$$\mathbf{\Phi}(i) = \left[\mathbf{J}^{-1}(\mathbf{\Phi}, \mathbf{y})\right]_{i,i}, \tag{3.48}$$

Chapter 4
Numerical Simulations

In this section, we illustrate the performance of our proposed EM-based multi-target estimator through numerical simulations. Towards this, we model the IO signal samples $\{x(n)\}$ with the first-order autoregressive AR(1) process [12]. We use a highly correlated waveform for IO with the AR(1) coefficient $\rho = -0.9$ and noise variance $\sigma^2 = 1 - |\rho|^2$. Thus, the process $\{x(n)\}$ has a unit average power and its auto-correlation function is given by $\eta(k) = (\rho)^{|k|}$, for any integer k. As discussed in section 3.1, we assume that the IO signal has a duration of T seconds and the receiver collects $N \geq \lfloor \frac{T}{T_s} + 1 \rfloor$ samples over the observation window by taking into account the maximum possible bistatic delay. So out of the total N samples collected, we take only $\lfloor \frac{T}{T_s} + 1 \rfloor$ of them as non-zero that are the IO signal samples and the remaining ones are zero. Thus, the IO waveform have the covariance matrix $\mathbf{R}_x$ as

$$\mathbf{R}_x = |\gamma|^2 \begin{bmatrix} \mathbf{R} & \mathbf{0} \\ \mathbf{0} & \mathbf{0} \end{bmatrix}, \tag{4.1}$$

where $|\gamma|^2$ represents magnitude-squared of the amplitude coefficient associated with the IO waveform. The (k, l) entry of the matrix $\mathbf{R}$ is given by $[\mathbf{R}]_{k,l} = \eta(k - l) \ \forall \ k, l = 1, \ldots, \lfloor \frac{T}{T_s} + 1 \rfloor$. Hence $\mathbf{\Sigma}_x = \mathbf{F}\mathbf{R}_x\mathbf{F}^H$ and for simplicity we take the noise covariance matrices as $\mathbf{\Sigma}_u = \sigma_u^2\mathbf{I}_N$ and $\mathbf{\Sigma}_v = \sigma_v^2\mathbf{I}_N$. The signal to noise ratio (SNR) for RC and SC are defined by

$$SNR_r = \frac{|\gamma|^2 \lfloor \frac{T}{T_s} + 1 \rfloor}{N\sigma_u^2}, \tag{4.2}$$

$$SNR_s = \frac{|\gamma|^2 \lfloor \frac{T}{T_s} + 1 \rfloor \sum_{m=1}^{M} |\alpha_m|^2}{NM\sigma_v^2}, \tag{4.3}$$

For the simulated cases below, we take $|\gamma|^2 = 1$, $N = 256$, $T = 201.8$ seconds, and $T_s = 1$ seconds (i.e., $f_s = 1$ Hertz). In order to measure the performance of considered estimators for estimating the delays and Doppler shifts of multiple targets, we define the mean squared

error (MSE) for the delays and Doppler shifts estimates by

$$\mathrm{MSE}_{\boldsymbol{\tau}} = \frac{1}{M}\sum_{m=1}^{M} \mathrm{E}[|\hat{\tau}_m - \tau_m|^2], \tag{4.4}$$

$$\mathrm{MSE}_{\mathbf{f}_d} = \frac{N^2}{M}\sum_{m=1}^{M} \mathrm{E}[|\hat{f}_m^d - f_m^d|^2], \tag{4.5}$$

where (4.4) and (4.5) are evaluated by using the Monte Carlo (MC) simulation method. In (4.5) we normalized the estimates of Doppler shifts by N, so $\mathrm{MSE}_{\mathbf{f}_d}$ can be interpreted as the performance metric with respect to the Fourier resolution of $1/N$. Note that, (4.4) and (4.5) represent the average of the MSEs' for individual delay and Doppler shift estimates, and therefore for each parameter, we accordingly plot the average of error variances which we get from computing the CRLB.

For the comparison purpose, we also study the performance of conventional CC estimator for estimating multiple targets in the environment. It is defined by [12] as

$$\left(\hat{\tau}_c, \hat{f}_c^d\right) = \arg\max_{(\tau_c, f_c^d)} \left|\mathbf{y}_s^H \mathbf{A}(f_c^d)\mathbf{W}(\tau_c)\mathbf{y}_r\right|, \tag{4.6}$$

where τ_c and f_c^d are the delay and Doppler shift parameters. In order to solve (4.6) and (3.24), we used Quasi-Newton algorithm from Matlab optimization toolbox with gradient of each cost function computed using (3.46) and (3.47).

For the following results we consider the scenario when two targets' reflected signals (i.e., $M = 2$) are captured in the SC where both component signal have the same SNR, i.e., $\alpha_1 = \alpha_2 = 1$. We consider two cases in this section. One is when both targets have widely separated delays and Doppler shifts (i.e., they are located far from each other and have different moving speeds), and the other case is when they have closely located delays and approximately the same Doppler shifts (i.e., they are closely located and have approximately the same moving speed).

4.1 Widely Separated Delays and Dopplers

First we start with this scenario and assume that the delays and Doppler shifts of the two targets are $[\tau_1, \tau_2]^T = [20.25, 33.75]^T$ and $\left[f_1^d, f_2^d\right]^T = [21.20/N, 34.11/N]^T$. In this case, the conventional CC cost function in (4.6) can visibly illustrate the two target peaks when evaluated over a wider delay-Doppler domain $[6, 18]$. Therefore, (4.6) can provide the distinct estimates for the delays and Doppler shifts of the two targets if solved twice from the initial point for each target. So, we compare next the MSE vs. SNR performance of CC in this multiple target scenario with our proposed EM-based multitarget estimator. Note that for the figures in this section 4.1 we averaged 100 MC trials and set the EM convergence coefficient to 10^{-6}.

Given a less noisy RC signal, i.e., with $SNR_r = 10$ dB, in Fig. 4.1 and 4.2 we first study the performance of both estimators with varying the quality of SC signal, i.e., SNR_s in the channel. We observe that at low SNR_s both estimators results in high MSE because of convergence to false noise peaks, whereas at high SNR_s our proposed EM-based multitarget estimator performs better than the CC estimator. Precisely, we can observe that the EM estimator converges to the CRLB with the increase in SNR_s, but the CC estimator does not converge. It is because for each target estimate by CC the other target acts as an interference to it, on the other hand, our EM algorithm breaks the composite SC signal into its respective signal components and uses the estimate of each one to estimate the respective target parameters as seen from the *Remark* in section 3.3.

Since the BPR uses a separate RC to capture the IO signal, it is highly expected that the performance of both estimators is a function of SNR in the RC. Thus, in Fig. 4.3 and 4.4, we evaluate the performance of both estimators with varying SNR_r when the $SNR_s = 0$ dB . It is observed that as the SNR_r decreases the performance of both estimators is also degraded, however, the EM estimator still outperforms the CC estimator. Also, if we compare Fig. 4.1, 4.2 with Fig. 4.3 and 4.4, respectively at $SNR_s = 0$ dB, we can see that when the SNR_r increases our EM estimator achieves the CRLB, but the CC

estimator fails on that. In addition to the above reasons, it is because our EM estimator uses the minimum MSE estimate of the IO signal for estimating the targets' parameters, whereas, the CC estimator works with the RC signal as the IO signal estimate.

4.2 Closely Located Delays and nearly same Dopplers

Next we study a worse case with a highly correlated IO waveform, i.e., when the two targets are closely located on a delay-Doppler plane. We consider one of the above considered environments, i.e., when $SNR_r = 10$ dB and $SNR_s = 5$ dB, and start with selecting the delays and Doppler shifts for the two targets as $[\tau_1, \tau_2]^T = [20.25, 22.10]^T$ and $\left[f_1^d, f_2^d\right]^T = [21.20/N, 21.32/N]^T$. Given approximately the same Doppler shifts, since the difference between the delays of the two targets is relatively smaller than the temporal correlation of the IO waveform, the conventional CC estimator in (4.6) can not distinguish the two targets as shown in Fig. 4.5. In Fig. 4.5, we show the location of true target coordinates as well as the only single estimate which we get by solving (4.6). Thus, CC can not be used for estimating the targets in this case, but since our proposed EM algorithm decomposes the composite SC signal into the respective target signals, it has two different cost surfaces (from (3.24)) for each target as shown in Fig. 4.6. To compare, in Fig. 4.6, we set up our EM algorithm with the target 1's delay and Doppler shift estimates initialized to the CC estimate shown in Fig. 4.5, and the target 2's delay and Doppler shift estimates initialized with a $+1$ and $+1/N$ perturbation to the CC's delay and Doppler shift estimate, respectively. The EM's convergence coefficient was set to 10^{-6} to get the EM estimates for the MC trial and we have plotted them on the EM surfaces at the converging iteration in the figure. From Fig. 4.6, we see that not only our proposed EM algorithm can separate the two closely located targets on the delay-Doppler plane but in fact it gives us two different delay and Doppler shift estimates corresponding to the two targets unlike the CC estimator.

To explore further, in Fig. 4.7 and 4.8, we study the average convergence performance of our proposed EM estimator under this considered case (b) starting from different initial points. We select two different initialization sets for our EM estimator through a coarse ML

search, i.e., set 1 contains $\tau_1^0 = 20.86$, $f_1^{d,0} = 22.16/N$, $\tau_2^0 = 22.80$, and $f_2^{d,0} = 22.11/N$, and set 2 contains $\tau_1^0 = 20.02$, $f_1^{d,0} = 20.94/N$, $\tau_2^0 = 21.95$, and $f_2^{d,0} = 20.99/N$. Note that set 1 defines a slightly bad initialization for our EM estimator as compared to set 2, and also that for the Fig. 4.7 and 4.8 we averaged 100 MC trials over all the iterations. The simulation results presented in Fig. 4.7 and 4.8 demonstrate that for both initialization settings, our proposed EM estimator converges in proximity to the CRLB in few iterations. Further, the convergence performance is a function of the initialization points, i.e., a good initial estimates results in a faster convergence of our proposed EM-based multitarget estimator.

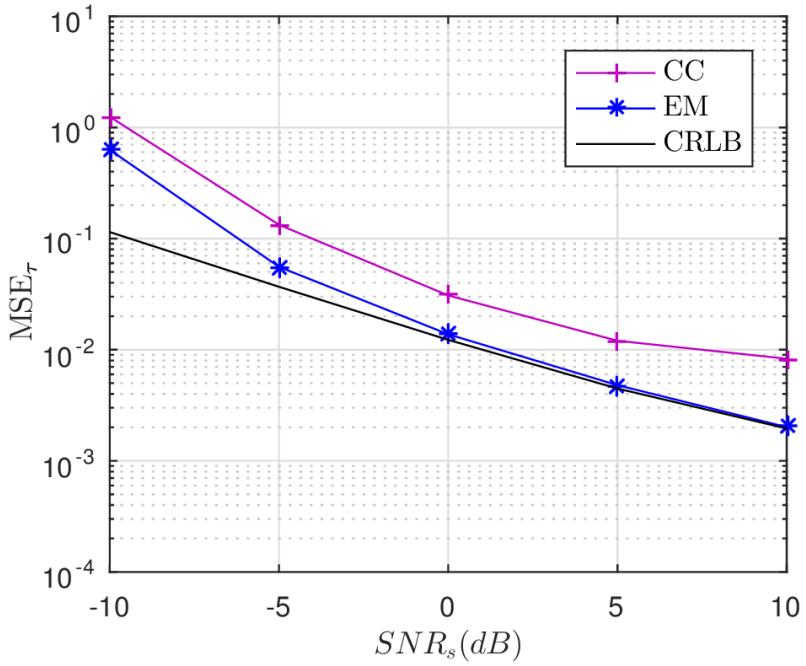

Figure 4.1: Estimators performance for estimating targets' bistatic delays with $SNR_r = 10$ dB

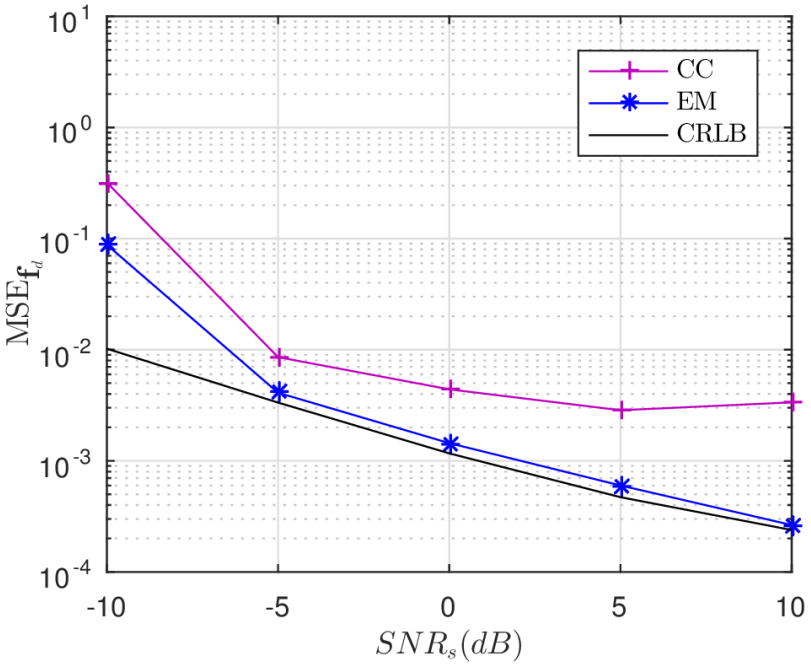

Figure 4.2: Estimators performance for estimating targets' Doppler shifts with $SNR_r = 10$ dB

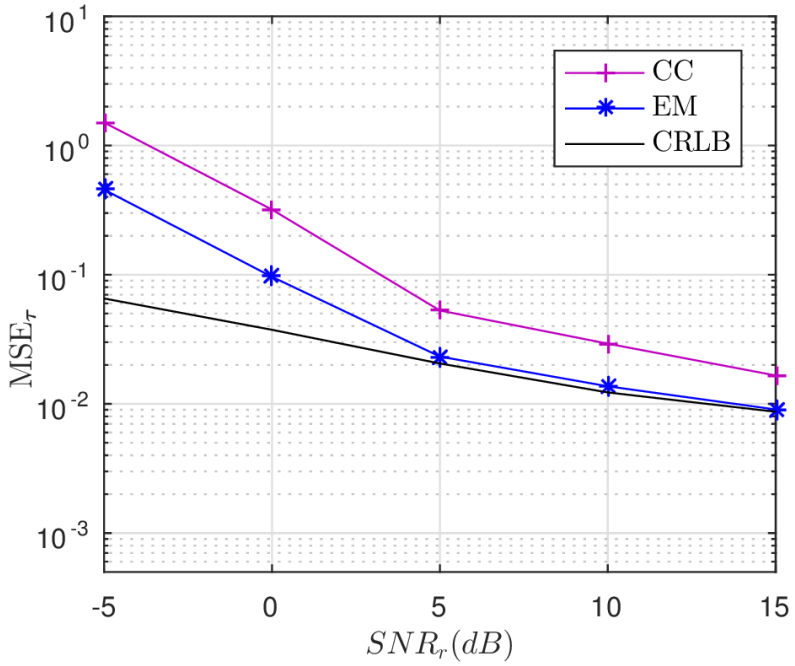

Figure 4.3: Estimators performance for estimating targets' bistatic delays with $SNR_s = 0$ dB

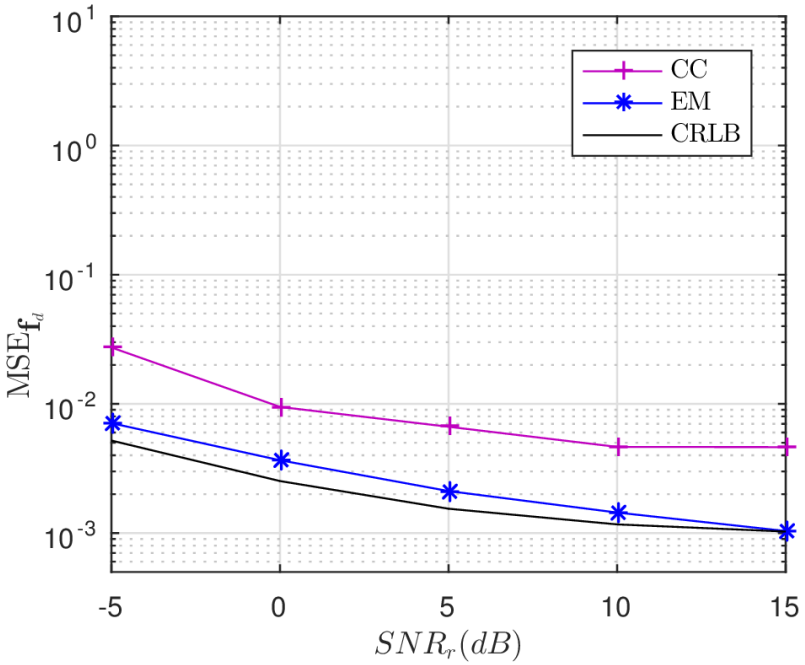

Figure 4.4: Estimators performance for estimating targets' Doppler shifts with $SNR_s = 0$ dB

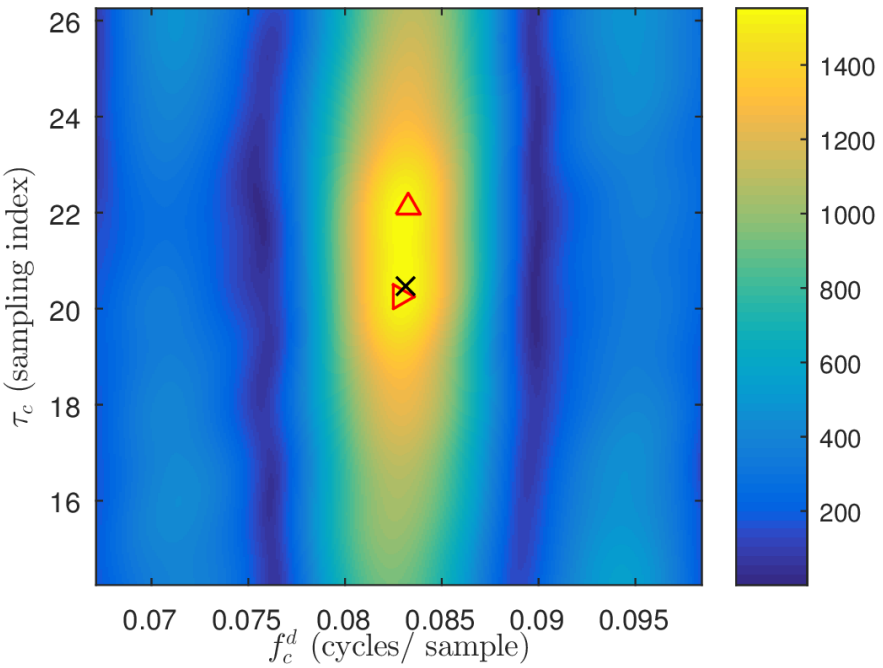

Figure 4.5: CC surface plot for section 4.2. Marks $\triangleright$ and $\triangle$ represent the true coordinates of the targets, and the mark $\times$ is at the CC estimated coordinates

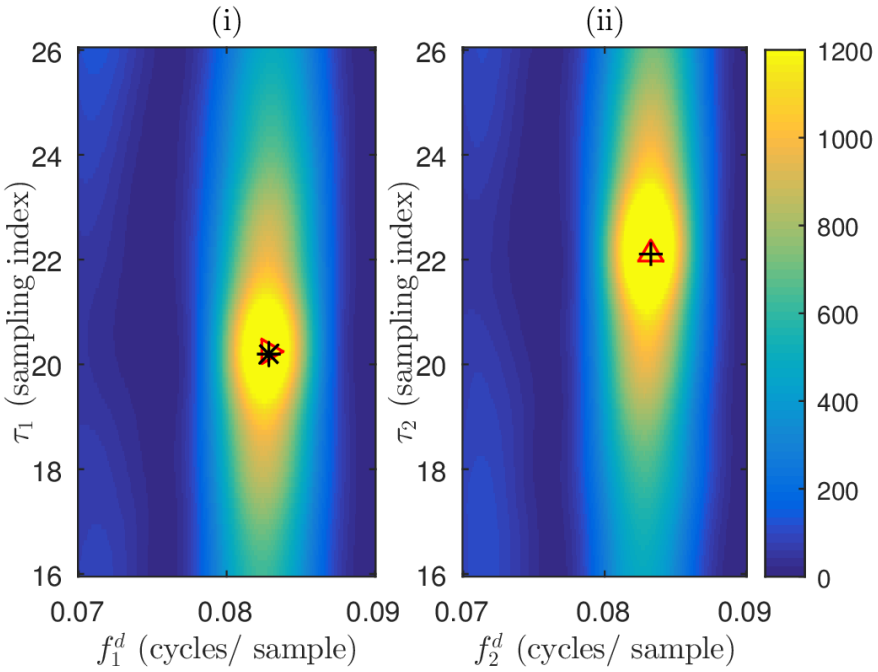

Figure 4.6: EM surfaces plot for section 4.2: (i) Target 1's EM surface with the true target coordinates at the mark $\triangleright$ and the EM estimated one at the mark $*$, (ii) Target 2's EM surface with the true target coordinates at the mark $\triangle$ and the EM estimated one at the mark $+$

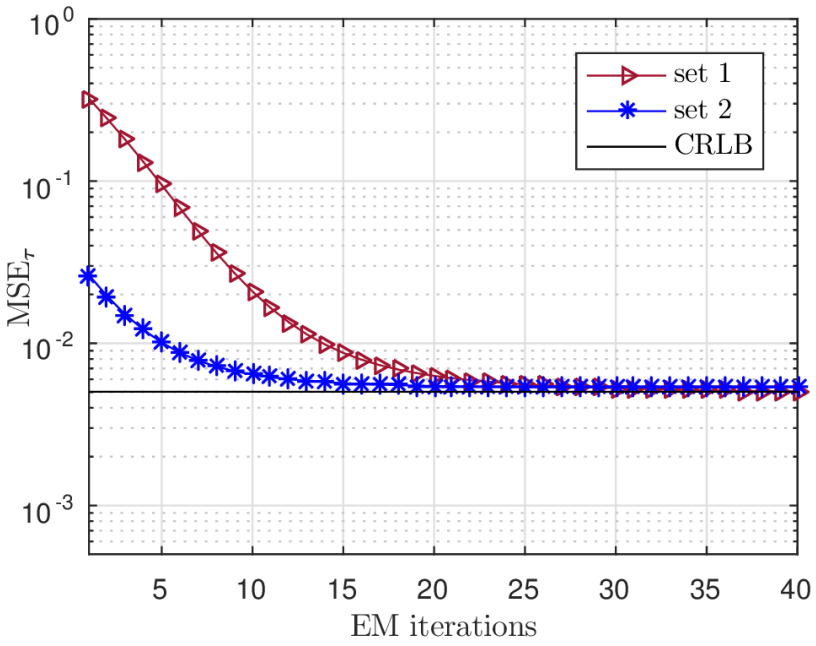

Figure 4.7: EM convergence performance for estimating targets' bistatic delays with $SNR_s = 5$ dB and $SNR_r = 10$ dB

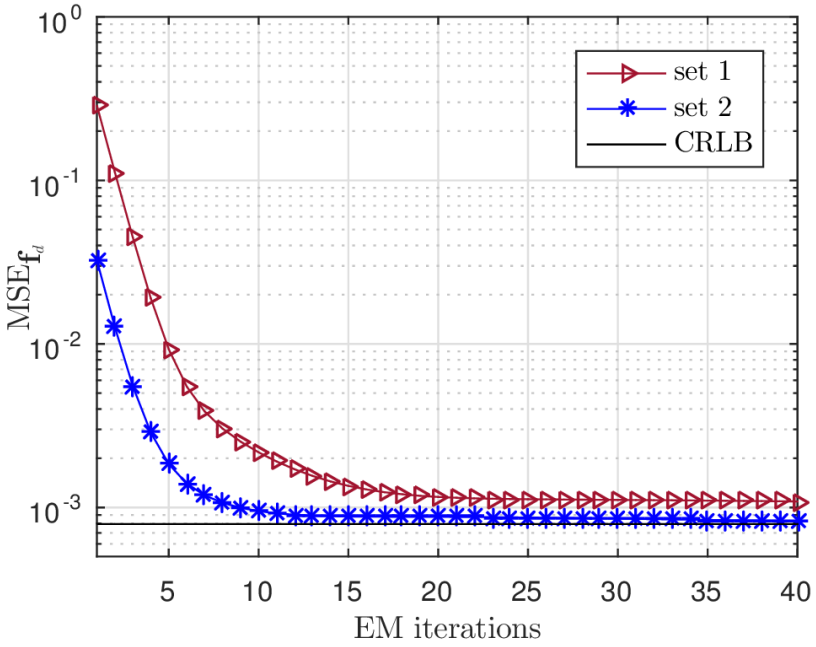

Figure 4.8: EM convergence performance for estimating targets' Doppler shifts with $SNR_s = 5$ dB and $SNR_r = 10$ dB

Chapter 5
Conclusion

In this thesis, we started with a brief background on passive radar and first reviewed the previous multiple target delay and Doppler shift estimation techniques in BPR systems, and the limitations in there. Taking into account the limitations of the previous work, we proposed a system model for estimating the delays and Doppler shifts of all the observed targets in a surveillance channel. Our system model treats all the delays and Doppler shifts as continuous-valued parameters and thereby avoids the straddle performance loss due to their discretization.

Given our two channel system model, we then considered the problem of jointly estimating the delays and Doppler shifts of all the observed targets in a SC when the IO signal is modeled as a correlated stochastic process. An ML estimator was identified as a possible solution for the posed problem, but its inherited multi-dimensional optimization approach increases the computational complexity of the estimator, and therefore, makes it less favorable. Therefore in this thesis, we proposed a computationally efficient EM-based multitarget estimator that breaks up the complex multi-dimensional ML optimization problem into multiple parallel single target optimization problems. The computational complexity of our proposed EM estimator remains unaffected with the increase in the number of observed targets by the SC. Furthermore, our EM estimator also provides the estimate of the unknown IO signal and the estimate of each target's component signal in SC, where this particularly later one can be used to remove the masking effect of strong targets for weak targets detection [34]. We also derived the CRLB to benchmark the performance of our proposed EM-based multitarget estimator. Numerical simulations were added to compare its performance with the widely used CC estimator. The results showed that for widely separated targets on a delay-Doppler plane, the performance of CC estimator did not achieve the CRLB with the increase in SNR_s due to the presence of interference from other targets, but our proposed multi-target EM estimator performed better than CC with increasing SNR_s and in fact very close to the CRLB. The CC estimator could not even

outperform our EM estimator when the RC was cleaner. Particularly, for the closely located targets on the delay-Doppler plane where the CC failed, our EM estimator was still functional and it could estimate the two targets in just few iterations with the estimation accuracy that was close to the CRLB.

References

[1] H. Sun, D. K. P. Tan, Y. Lu, and M. Lesturgie, "Applications of passive surveillance radar system using cell phone base station illuminators," *IEEE Aerospace and Electronic Systems Magazine*, vol. 25, pp. 10–18, March 2010.

[2] P. E. Howland, D. Maksimiuk, and G. Reitsma, "Fm radio based bistatic radar," *IEEE Proceedings - Radar, Sonar and Navigation*, vol. 152, pp. 107–115, June 2005.

[3] D. Poullin, "Passive detection using digital broadcasters (dab, dvb) with cofdm modulation," *IEEE Proceedings - Radar, Sonar and Navigation*, vol. 152, pp. 143–152, June 2005.

[4] H. D. Griffiths and C. J. Baker, "Passive coherent location radar systems. part 1: performance prediction," *IEE Proceedings - Radar, Sonar and Navigation*, vol. 152, pp. 153–159, June 2005.

[5] N. J. Willis and H. Griffiths, *Advances in bistatic radar*. Raleigh, NC : SciTech Pub., c2007, 2nd ed., 2007.

[6] K. Kulpa, M. Malanowski, J. Misiurewicz, and P. Samczynski, "Passive radar for strategic object protection," in *2011 IEEE International Conference on Microwaves, Communications, Antennas and Electronic Systems (COMCAS 2011)*, pp. 1–4, Nov 2011.

[7] J. Liu, H. Li, and B. Himed, "On the performance of the cross-correlation detector for passive radar applications," *Signal Process.*, vol. 113, pp. 32–37, Aug. 2015.

[8] G. Cui, J. Liu, H. Li, and B. Himed, "Target detection for passive radar with noisy reference channel," in *2014 IEEE Radar Conference*, pp. 0144–0148, May 2014.

[9] S. Gogineni, P. Setlur, M. Rangaswamy, and R. R. Nadakuditi, "Random matrix theory inspired passive bistatic radar detection with noisy reference signal," in *2015 IEEE International Conference on Acoustics, Speech and Signal Processing (ICASSP)*, pp. 2754–2758, April 2015.

[10] J. Liu, H. Li, and B. Himed, "Two target detection algorithms for passive multistatic radar," *IEEE Transactions on Signal Processing*, vol. 62, pp. 5930–5939, Nov 2014.

[11] D. Cochran, H. Gish, and D. Sinno, "A geometric approach to multiple-channel signal detection," *IEEE Transactions on Signal Processing*, vol. 43, pp. 2049–2057, Sep 1995.

[12] X. Zhang, H. Li, J. Liu, and B. Himed, "Joint delay and doppler estimation for passive sensing with direct-path interference," *IEEE Transactions on Signal Processing*, vol. 64, pp. 630–640, Feb 2016.

[13] X. Zhang, H. Li, and B. Himed, "Multistatic detection for passive radar with direct-path interference," *IEEE Transactions on Aerospace and Electronic Systems*, vol. 53, pp. 915–925, April 2017.

[14] M. Malanowski and K. Kulpa, "Digital beamforming for passive coherent location radar," in *2008 IEEE Radar Conference*, pp. 1–6, May 2008.

[15] R. Tao, H. Z. Wu, and T. Shan, "Direct-path suppression by spatial filtering in digital television terrestrial broadcasting-based passive radar," *IET Radar, Sonar Navigation*, vol. 4, pp. 791–805, December 2010.

[16] J. L. Garry, G. E. Smith, and C. J. Baker, "Direct signal suppression schemes for passive radar," in *2015 Signal Processing Symposium (SPSympo)*, pp. 1–5, June 2015.

[17] C. Schwark and D. Cristallini, "Advanced multipath clutter cancellation in ofdm-based passive radar systems," in *2016 IEEE Radar Conference (RadarConf)*, pp. 1–4, May 2016.

[18] R. S. A. R. Abdullah, A. A. Salah, and N. E. A. Rashid, "Moving target detection by using new lte-based passive radar," *Progress in Electromagnetic Research B*, vol. 63, pp. 145–160, 2015.

[19] F. Colone, D. W. O'Hagan, P. Lombardo, and C. J. Baker, "A multistage processing algorithm for disturbance removal and target detection in passive bistatic radar," *IEEE Transactions on Aerospace and Electronic Systems*, vol. 45, pp. 698–722, April 2009.

[20] S. Subedi, Y. D. Zhang, M. G. Amin, and B. Himed, "Group sparsity based multi-target tracking in passive multi-static radar systems using doppler-only measurements," *IEEE Transactions on Signal Processing*, vol. 64, pp. 3619–3634, July 2016.

[21] A. Zaimbashi, M. Derakhtian, and A. Sheikhi, "Glrt-based cfar detection in passive bistatic radar," *IEEE Transactions on Aerospace and Electronic Systems*, vol. 49, pp. 134–159, Jan 2013.

[22] A. Zaimbashi, "Forward m-ary hypothesis testing based detection approach for passive radar," *IEEE Transactions on Signal Processing*, vol. 65, pp. 2659–2671, May 2017.

[23] A. Zaimbashi, "Target detection in analog terrestrial tv-based passive radar sensor: Joint delay-doppler estimation," *IEEE Sensors Journal*, vol. 17, pp. 5569–5580, Sept 2017.

[24] G. Cui, J. Liu, H. Li, and B. Himed, "Signal detection with noisy reference for passive sensing," *Signal Processing*, vol. 108, no. Supplement C, pp. 389 – 399, 2015.

[25] S. P. Belanger, "An em algorithm for multisensor tdoa/dd estimation in a multi-path propagation environment," in *1996 IEEE International Conference on Acoustics, Speech, and Signal Processing Conference Proceedings*, vol. 6, pp. 3117–3120 vol. 6, May 1996.

[26] P. Stoica and Y. Selen, "Model-order selection: a review of information criterion rules," *IEEE Signal Processing Magazine*, vol. 21, pp. 36–47, July 2004.

[27] Z. Zhu and S. Kay, "On bayesian exponentially embedded family for model order selection," *IEEE Transactions on Signal Processing*, vol. 66, pp. 933–943, Feb 2018.

[28] T. Hwang, C. Yang, G. Wu, S. Li, and G. Y. Li, "Ofdm and its wireless applications: A survey," *IEEE Transactions on Vehicular Technology*, vol. 58, pp. 1673–1694, May 2009.

[29] W. B. Davenport, *Probability and random processes: an introduction for applied scientists and engineers*. New York:McGraw-Hill, 1987.

[30] F. Pourkamali-Anaraki, "Estimation of the sample covariance matrix from compressive measurements," *IET Signal Processing*, vol. 10, no. 9, pp. 1089–1095, 2016.

[31] S. K. Mitra, *Digital Signal Processing: A Computer-Based Approach*. McGraw-Hill School Education Group, 2nd ed., 2001.

[32] A. P. Dempster, N. M. Laird, and D. B. Rubin, "Maximum likelihood from incomplete data via the em algorithm," *Journal of the Royal Statistical Society, Series B*, vol. 39, no. 1, pp. 1–38, 1977.

[33] S. Boyd and L. Vandenberghe, *Convex Optimization*. New York, NY, USA: Cambridge University Press, 2004.

[34] K. S. Kulpa and Z. Czekala, "Masking effect and its removal in pcl radar," *IEE Proceedings - Radar, Sonar and Navigation*, vol. 152, pp. 174–178, June 2005.

[35] S. M. Kay, *Fundamentals of Statistical Signal Processing: Estimation Theory*. Upper Saddle River, NJ, USA: Prentice-Hall, 1993.

[36] G. A. F. Seber, *A matrix handbook for statisticians*. Hoboken, N.J. : Wiley-Interscience, c2008., 2008.

[37] L. L. Scharf, *Statistical Signal Processing. Detection, Estimation, and Times Series Analysis*. Addison-Wesley, 1991.

Appendix A
Solving (3.19)

Using the assumption of section 3.1, the log-likelihood function of the complete data $\mathbf{h} = [\mathbf{z}^T, \mathbf{x}^T]^T$ is given by

$$\begin{aligned} L(\boldsymbol{\Theta}; \mathbf{h}) &= \ln p(\mathbf{h}|\boldsymbol{\Theta}) = \ln\, [p(\mathbf{z}|\boldsymbol{\Theta}, \mathbf{x}) p(\mathbf{x})] \\ &= \ln \left(\prod_{m=1}^{M} p(\mathbf{z}_m|\boldsymbol{\theta}_m, \mathbf{x}) p(\mathbf{x}) \right) \\ &= r_1 - \sum_{m=1}^{M} \big[(\mathbf{z}_m - \boldsymbol{\Gamma}_1(\boldsymbol{\theta}_m)\mathbf{x})^H (\boldsymbol{\Sigma}_v^m)^{-1} \times \\ &\qquad\qquad (\mathbf{z}_m - \boldsymbol{\Gamma}_1(\boldsymbol{\theta}_m)\mathbf{x}) \big] \\ &= r_2 + \sum_{m=1}^{M} \big[2\Re \left\{ \mathbf{z}_m^H (\boldsymbol{\Sigma}_v^m)^{-1} \left(\boldsymbol{\Gamma}_1(\boldsymbol{\theta}_m)\mathbf{x} \right) \right\} - \\ &\quad |\alpha_m|^2 \left(\boldsymbol{\Gamma}_0 \left(f_m^d, \tau_m \right) \mathbf{x} \right)^H (\boldsymbol{\Sigma}_v^m)^{-1} \left(\boldsymbol{\Gamma}_0 \left(f_m^d, \tau_m \right) \mathbf{x} \right) \big], \end{aligned} \tag{A.1}$$

where the constant r_1 and r_2 contains the terms that are independent of $\boldsymbol{\Theta}$, and the matrix $\boldsymbol{\Gamma}_1(\boldsymbol{\theta}_m) = \alpha_m \boldsymbol{\Gamma}_0 \left(f_m^d, \tau_m \right)$ with $\boldsymbol{\Gamma}_0 \left(f_m^d, \tau_m \right) = \mathbf{A}(f_m^d)\mathbf{W}(\tau_m)$. So the required cost function in (3.19) is thus given by

$$\begin{aligned} Q(\boldsymbol{\Theta}; \boldsymbol{\Theta}^p) &= E[L(\boldsymbol{\Theta}; \mathbf{h}) \mid \mathbf{y}, \boldsymbol{\Theta}^p] \\ &= r_3 + \sum_{m=1}^{M} \Big[2\Re \left\{ \alpha_m \mathrm{tr} \left\{ \boldsymbol{\Gamma}_2 \left(f_m^d, \tau_m \right) \boldsymbol{\Sigma}_{xz|y}^{m,p} \right\} \right\} \\ &\quad - |\alpha_m|^2 \mathrm{tr} \left\{ \boldsymbol{\Gamma}_2 \left(f_m^d, \tau_m \right) \boldsymbol{\Sigma}_{xx|y}^{p} \boldsymbol{\Gamma}_0^H \left(f_m^d, \tau_m \right) \right\} \Big], \end{aligned} \tag{A.2}$$

where r_3 represents the terms that are not a function of $\boldsymbol{\Theta}$ and the matrix $\boldsymbol{\Gamma}_2 \left(f_m^d, \tau_m \right) = (\boldsymbol{\Sigma}_v^m)^{-1} \boldsymbol{\Gamma}_0 \left(f_m^d, \tau_m \right)$. The conditional covariance matrices $\boldsymbol{\Sigma}_{xz|y}^{m,p}$ and $\boldsymbol{\Sigma}_{xx|y}^{p}$ in (A.2) can be obtained by using the fact that $\mathbf{x}$, $\mathbf{z}_m$, and $\mathbf{y}$ are jointly Gaussian, so by (B.10) of Appendix

B the vectors $\mathbf{x}^p$ and $\mathbf{z}_m^p$ have the following closed form expressions

$$\mathbf{x}^p = E[\mathbf{x} \mid \mathbf{y}, \boldsymbol{\Theta}^p] = \boldsymbol{\Sigma}_{xy}^p \left(\boldsymbol{\Sigma}_y^p\right)^{-1} \mathbf{y}, \tag{A.3}$$

$$\mathbf{z}_m^p = E[\mathbf{z}_m \mid \mathbf{y}, \boldsymbol{\Theta}^p] = \boldsymbol{\Sigma}_{zy}^{m,p} \left(\boldsymbol{\Sigma}_y^p\right)^{-1} \mathbf{y}, \tag{A.4}$$

where the matrices $\boldsymbol{\Sigma}_y^p$, $\boldsymbol{\Sigma}_{xy}^p$, and $\boldsymbol{\Sigma}_{zy}^{m,p}$ are evaluated by using the p^{th} estimate of the parameter set $\boldsymbol{\Theta}$ in (3.11)-(3.14) and (B.5)-(B.6). Next using (3.11), (B.5), and (B.6) along with the block matrix inversion formula from [36], we can simplify (A.3) and (A.4) to

$$\mathbf{x}^p = \mathbf{y}_r - \boldsymbol{\Sigma}_u \mathbf{K}_0^{-1} \mathbf{y}_r + \boldsymbol{\Sigma}_u \mathbf{D}^{-1} \mathbf{P}(\boldsymbol{\Theta}^p) \mathbf{K}_1^{-1} \mathbf{y}_s, \tag{A.5}$$

$$\mathbf{z}_m^p = \boldsymbol{\Gamma}_1 \left(\boldsymbol{\theta}_m^p\right) \mathbf{x}^p + \boldsymbol{\Sigma}_v^m \left[\mathbf{K}_1^{-1} \mathbf{y}_s - \mathbf{K}_1^{-1} \mathbf{P}^H(\boldsymbol{\Theta}^p) \mathbf{D}^{-1} \mathbf{y}_r\right], \tag{A.6}$$

where $\mathbf{K}_0$ and $\mathbf{K}_1$ are the Schur complements defined as

$$\mathbf{K}_0 = \mathbf{D} - \mathbf{P}(\boldsymbol{\Theta}^p) \mathbf{B}^{-1}(\boldsymbol{\Theta}^p) \mathbf{P}^H(\boldsymbol{\Theta}^p), \tag{A.7}$$

$$\mathbf{K}_1 = \mathbf{B} - \mathbf{P}^H(\boldsymbol{\Theta}^p) \mathbf{D}^{-1} \mathbf{P}(\boldsymbol{\Theta}^p), \tag{A.8}$$

Note that (A.5) and (A.6) estimates the IO signal and the m^{th} component in the SC signal, respectively. Thus using (A.3) and (A.4) along with $\boldsymbol{\Gamma}_{xx|y}(\boldsymbol{\Theta})$ and $\boldsymbol{\Gamma}_{xz|y}(\boldsymbol{\Theta})$ from (B.12) and (B.13) of Appendix B, the conditional covariance matrices used in (A.2) are given by

$$\begin{aligned} \boldsymbol{\Sigma}_{xx|y}^p &= E[\mathbf{x}\mathbf{x}^H \mid \mathbf{y}, \boldsymbol{\Theta}^p] \\ &= \mathbf{x}^p (\mathbf{x}^p)^H + \boldsymbol{\Gamma}_{xx|y}(\boldsymbol{\Theta}^p) \\ &= \mathbf{x}^p (\mathbf{x}^p)^H + \boldsymbol{\Sigma}_x - \boldsymbol{\Sigma}_{xy}^p \left(\boldsymbol{\Sigma}_y^p\right)^{-1} \left(\boldsymbol{\Sigma}_{xy}^p\right)^H \\ &= \mathbf{x}^p (\mathbf{x}^p)^H + \boldsymbol{\Sigma}_u - \boldsymbol{\Sigma}_u \mathbf{K}_0^{-1} \boldsymbol{\Sigma}_u, \end{aligned} \tag{A.9}$$

$$
\begin{aligned}
\boldsymbol{\Sigma}_{xz|y}^{m,p} &= E[\mathbf{x}(\mathbf{z}_m)^H \mid \mathbf{y}, \boldsymbol{\Theta}^p] \\
&= \mathbf{x}^p \left(\mathbf{z}_m^p\right)^H + \boldsymbol{\Gamma}_{xz|y}(\boldsymbol{\Theta}^p) \\
&= \mathbf{x}^p (\mathbf{z}_m^p)^H + \boldsymbol{\Sigma}_x \boldsymbol{\Gamma}_1^H \left(\boldsymbol{\theta}_m^p\right) - \boldsymbol{\Sigma}_{xy}^p \left(\boldsymbol{\Sigma}_y^p\right)^{-1} \left(\boldsymbol{\Sigma}_{zy}^{m,p}\right)^H \\
&= \mathbf{x}^p (\mathbf{z}_m^p)^H + \boldsymbol{\Sigma}_u \boldsymbol{\Gamma}_1^H \left(\boldsymbol{\theta}_m^p\right) - \boldsymbol{\Sigma}_u \mathbf{K}_0^{-1} \boldsymbol{\Sigma}_u \boldsymbol{\Gamma}_1^H (\boldsymbol{\theta}_m^p) \\
&\quad - \boldsymbol{\Sigma}_u \mathbf{D}^{-1} \mathbf{P}(\boldsymbol{\Theta}^p) \mathbf{K}_1^{-1} \boldsymbol{\Sigma}_v^m,
\end{aligned}
\tag{A.10}
$$

where and the fourth equality in (A.9) and (A.10) is obtained by using the block matrix inversion formula [36] along with (3.11), (B.5), and (B.6).

Appendix B
Computing conditional means in (A.3) and (A.4)

Here we derive equations to find the conditional means in (A.3) and (A.4) and the conditional covariance matrices $\mathbf{\Gamma}_{xx|y}$ and $\mathbf{\Gamma}_{xz|y}$ in the second equality of (A.9) and (A.10). So lets define $\mathbf{h}_m = [\mathbf{x}^T, \mathbf{z}_m^T]^T$ then $\mathbf{h}_m$ has circularly symmetric complex Gaussian distribution with zero mean and covariance matrix $\mathbf{\Sigma}_{hh}^m$ given as

$$\begin{aligned}\mathbf{\Sigma}_{hh}^m &= \mathrm{E}[\mathbf{h}_m \mathbf{h}_m^H] \\ &= \begin{bmatrix} \mathbf{\Sigma}_x & \mathbf{\Sigma}_{xz}^m(\boldsymbol{\theta}_m) \\ (\mathbf{\Sigma}_{xz}^m(\boldsymbol{\theta}_m))^H & \mathbf{\Sigma}_z^m(\boldsymbol{\theta}_m) \end{bmatrix},\end{aligned} \tag{B.1}$$

where

$$\mathbf{\Sigma}_{xz}^m(\boldsymbol{\theta}_m) = \mathrm{E}[\mathbf{x}\mathbf{z}_m^H] = \mathbf{\Sigma}_x \mathbf{\Gamma}_1^H(\boldsymbol{\theta}_m), \tag{B.2}$$

$$\mathbf{\Sigma}_z^m(\boldsymbol{\theta}_m) = \mathrm{E}[\mathbf{z}_m \mathbf{z}_m^H] = \mathbf{\Gamma}_1(\boldsymbol{\theta}_m)\mathbf{\Sigma}_x \mathbf{\Gamma}_1^H(\boldsymbol{\theta}_m) + \mathbf{\Sigma}_v^m, \tag{B.3}$$

The matrix $\mathbf{\Gamma}_1(\boldsymbol{\theta}_m)$ and $\mathbf{\Gamma}_0\left(f_m^d, \tau_m\right)$ are defined in Appendix A. The vector $\mathbf{h}_y^m = [\mathbf{h}_m^T, \mathbf{y}^T]^T$ has a circularly symmetric complex Gaussian distribution with zero mean and covariance matrix $\mathbf{\Sigma}_{hy}^m(\mathbf{\Theta})$ given as

$$\begin{aligned}\mathbf{\Sigma}_{hy}^m(\mathbf{\Theta}) &= \mathrm{E}[\mathbf{h}_y^m (\mathbf{h}_y^m)^H] \\ &= \begin{bmatrix} \mathbf{\Sigma}_{hh}^m & \mathbf{\Sigma}_{xyz}^m(\mathbf{\Theta}) \\ \left(\mathbf{\Sigma}_{xyz}^m(\mathbf{\Theta})\right)^H & \mathbf{\Sigma}_y(\mathbf{\Theta}) \end{bmatrix},\end{aligned} \tag{B.4}$$

where $\mathbf{\Sigma}_{xyz}^m(\mathbf{\Theta}) = \begin{bmatrix} (\mathbf{\Sigma}_{xy}(\mathbf{\Theta}))^T & \left(\mathbf{\Sigma}_{zy}^m(\mathbf{\Theta})\right)^T \end{bmatrix}^T$ with

$$\mathbf{\Sigma}_{xy}(\mathbf{\Theta}) = \mathrm{E}[\mathbf{x}\mathbf{y}^H] = [\mathbf{\Sigma}_x \quad \mathbf{P}(\mathbf{\Theta})], \tag{B.5}$$

$$\mathbf{\Sigma}_{zy}^m(\mathbf{\Theta}) = \mathrm{E}[\mathbf{z}_m \mathbf{y}^H] = [\mathbf{\Gamma}_1(\boldsymbol{\theta}_m)\mathbf{\Sigma}_x \quad \mathbf{\Gamma}_1(\boldsymbol{\theta}_m)\mathbf{P}(\mathbf{\Theta}) + \mathbf{\Sigma}_v^m], \tag{B.6}$$

and with $\mathbf{\Sigma}_x$ and $\mathbf{\Sigma}_y(\mathbf{\Theta})$ as defined in section 3.1. Now given the observation vector $\mathbf{y}$ and $\mathbf{\Theta}$ we are interested to estimate $\mathbf{h}_m$, so we find the conditional distribution of $\mathbf{h}_m$ given $\mathbf{y}$ as

$$\begin{aligned} p(\mathbf{h}_m \mid \mathbf{y}, \mathbf{\Theta}) &= \frac{p(\mathbf{h}_m, \mathbf{y} \mid \mathbf{\Theta})}{p(\mathbf{y} \mid \mathbf{\Theta})} \\ &= \frac{\det\{\pi \mathbf{\Sigma}_{hy}^m(\mathbf{\Theta})\}^{-1} \exp\left[-(\mathbf{h}_y^m)^H \left(\mathbf{\Sigma}_{hy}^m(\mathbf{\Theta})\right)^{-1} \mathbf{h}_y^m\right]}{\det\{\pi \mathbf{\Sigma}_y(\mathbf{\Theta})\}^{-1} \exp\left[-\mathbf{y}^H \left(\mathbf{\Sigma}_y(\mathbf{\Theta})\right)^{-1} \mathbf{y}\right]}, \end{aligned} \tag{B.7}$$

where to find the inverse of $\mathbf{\Sigma}_{hy}^m(\mathbf{\Theta})$ we use the second equality from (7.75) in [37, p. 294] to get

$$\begin{aligned} \left(\mathbf{\Sigma}_{hy}^m(\mathbf{\Theta})\right)^{-1} = &\begin{bmatrix} \mathbf{0}_{2N\times 2N} & \mathbf{0}_{2N\times 2N} \\ \mathbf{0}_{2N\times 2N} & \mathbf{\Sigma}_y^{-1}(\mathbf{\Theta}) \end{bmatrix} + \\ &\begin{bmatrix} \mathbf{I} \\ -\mathbf{\Sigma}_y^{-1}(\mathbf{\Theta}) \left(\mathbf{\Sigma}_{xyz}^m(\mathbf{\Theta})\right)^H \end{bmatrix} (\mathbf{K}^{'})^{-1} \begin{bmatrix} \mathbf{I} & -\mathbf{\Sigma}_{xyz}^m(\mathbf{\Theta}) \mathbf{\Sigma}_y^{-1}(\mathbf{\Theta}) \end{bmatrix}, \end{aligned} \tag{B.8}$$

and using it we solve (B.7) to obtain

$$\begin{aligned} p(\mathbf{h}_m \mid \mathbf{y}, \mathbf{\Theta}) = \det\{\pi \mathbf{K}^{'}\}^{-1} \exp\Big\{ &- \left(\mathbf{h}_m - \hat{\mathbf{h}}_m\right)^H \left(\mathbf{K}^{'}\right)^{-1} \times \\ &\left(\mathbf{h}_m - \hat{\mathbf{h}}_m\right) \Big\}, \end{aligned} \tag{B.9}$$

where the required mean $\hat{\mathbf{h}}_m$ and the covariance matrix $\mathbf{K}^{'}$ of (B.9) is

$$\hat{\mathbf{h}}_m = \begin{bmatrix} \hat{\mathbf{x}} \\ \hat{\mathbf{z}}_m \end{bmatrix} = \begin{bmatrix} \mathbf{\Sigma}_{xy}(\mathbf{\Theta}) \mathbf{\Sigma}_y^{-1}(\mathbf{\Theta}) \mathbf{y} \\ \mathbf{\Sigma}_{zy}^m(\mathbf{\Theta}) \mathbf{\Sigma}_y^{-1}(\mathbf{\Theta}) \mathbf{y} \end{bmatrix}, \tag{B.10}$$

$$\begin{aligned} \mathbf{K}^{'} &= \mathbf{\Sigma}_{hh}^m(\boldsymbol{\theta}_m) - \mathbf{\Sigma}_{xyz}^m \mathbf{\Sigma}_y^{-1}(\mathbf{\Theta}) \left(\mathbf{\Sigma}_{xyz}^m\right)^H \\ &= \begin{bmatrix} \mathbf{\Gamma}_{xx|y}(\mathbf{\Theta}) & \mathbf{\Gamma}_{xz|y}(\mathbf{\Theta}) \\ \mathbf{\Gamma}_{xz|y}^H(\mathbf{\Theta}) & \mathbf{\Gamma}_{zz|y}(\mathbf{\Theta}) \end{bmatrix}, \end{aligned} \tag{B.11}$$

with

$$\begin{aligned}
\boldsymbol{\Gamma}_{xx|y}(\boldsymbol{\Theta}) &= \mathrm{E}[(\mathbf{x}-\hat{\mathbf{x}})(\mathbf{x}-\hat{\mathbf{x}})^H \mid \mathbf{y}, \boldsymbol{\Theta}] \\
&= \boldsymbol{\Sigma}_x - \boldsymbol{\Sigma}_{xy}(\boldsymbol{\Theta})\boldsymbol{\Sigma}_y^{-1}(\boldsymbol{\Theta})\boldsymbol{\Sigma}_{xy}^H(\boldsymbol{\Theta}), \qquad \text{(B.12)} \\
\boldsymbol{\Gamma}_{xz|y}(\boldsymbol{\Theta}) &= \mathrm{E}[(\mathbf{x}-\hat{\mathbf{x}})(\mathbf{z}_m-\hat{\mathbf{z}}_m)^H \mid \mathbf{y}, \boldsymbol{\Theta}] \\
&= \boldsymbol{\Sigma}_{xz}^m(\boldsymbol{\Theta}) - \boldsymbol{\Sigma}_{xy}(\boldsymbol{\Theta})\boldsymbol{\Sigma}_y^{-1}(\boldsymbol{\Theta})\left(\boldsymbol{\Sigma}_{zy}^m(\boldsymbol{\Theta})\right)^H, \qquad \text{(B.13)} \\
\boldsymbol{\Gamma}_{zz|y}(\boldsymbol{\Theta}) &= \mathrm{E}[(\mathbf{z}_m-\hat{\mathbf{z}}_m)(\mathbf{z}_m-\hat{\mathbf{z}}_m)^H \mid \mathbf{y}, \boldsymbol{\Theta}] \\
&= \boldsymbol{\Sigma}_z^m(\boldsymbol{\theta}_m) - \boldsymbol{\Sigma}_{zy}^m(\boldsymbol{\Theta})\boldsymbol{\Sigma}_y^{-1}(\boldsymbol{\Theta})\left(\boldsymbol{\Sigma}_{zy}^m(\boldsymbol{\Theta})\right)^H, \qquad \text{(B.14)}
\end{aligned}$$

Appendix C
Deriving (3.26) and (3.27)

As the EM algorithm in section 3.3 converges, we obtain (i) $\tau_m^{p+1} \approx \tau_m^p$, (ii) $f_m^{d,p+1} \approx f_m^{d,p}$, (iii) $\mathbf{\Sigma}_{xx|y}^p \approx \mathbf{x}^p \left(\mathbf{x}^p\right)^H$, and (iv) $\mathbf{\Sigma}_{xz|y}^{m,p} \approx \mathbf{x}^p \left(\mathbf{z}_m^p\right)^H$. So given an estimate of α_m from p^{th} iteration, the optimization over (τ_m, f_m^d) using (3.21) can be approximated by

$$\begin{aligned}\left(\tau_m^{p+1}, f_m^{d,p+1}\right) &= \arg \max_{(\tau_m, f_m^d)} Q_1\left(\tau_m, f_m^d, \alpha_m^p; \mathbf{\Theta}^p\right) \\ &\approx \arg \max_{(\tau_m, f_m^d)} \mathbf{\Gamma}_3(f_m^d, \tau_m),\end{aligned} \tag{C.1}$$

where the approximation results by using (iii) and (iv) in (3.22) to get $\mathbf{\Gamma}_3(f_m^d, \tau_m)$ as follow

$$\begin{aligned}&\mathbf{\Gamma}_3(f_m^d, \tau_m) \\ &= 2\Re\left\{\left(\mathbf{z}_m^p\right)^H \left(\mathbf{\Sigma}_v^m\right)^{-1}\left(\alpha_m^p \mathbf{\Gamma}_0(f_m^d, \tau_m)\mathbf{x}^p\right)\right\} \\ &\quad - \left(\alpha_m^p \mathbf{\Gamma}_0(f_m^d, \tau_m)\mathbf{x}^p\right)^H \left(\mathbf{\Sigma}_v^m\right)^{-1}\left(\alpha_m^p \mathbf{\Gamma}_0(f_m^d, \tau_m)\mathbf{x}^p\right) \\ &= 2\Re\left\{\left[\left(\mathbf{\Sigma}_v^m\right)^{-1/2} \mathbf{z}_m^p\right]^H \left[\left(\mathbf{\Sigma}_v^m\right)^{-1/2}\left(\alpha_m^p \mathbf{\Gamma}_0(f_m^d, \tau_m)\mathbf{x}^p\right)\right]\right\} \\ &\quad - \left|\left|\left(\mathbf{\Sigma}_v^m\right)^{-1/2}\left(\alpha_m^p \mathbf{\Gamma}_0(f_m^d, \tau_m)\mathbf{x}^p\right)\right|\right|^2 \\ &= \left|\left|\left(\mathbf{\Sigma}_v^m\right)^{-1/2} \mathbf{z}_m^p\right|\right|^2 \\ &\quad - \left|\left|\left(\mathbf{\Sigma}_v^m\right)^{-1/2}\left(\mathbf{z}_m^p - \alpha_m^p \mathbf{\Gamma}_0(f_m^d, \tau_m)\mathbf{x}^p\right)\right|\right|^2,\end{aligned} \tag{C.2}$$

by putting $\mathbf{\Gamma}_0(f_m^d, \tau_m) = \mathbf{A}(f_m^d)\mathbf{W}(\tau_m)$ in the last equality of (C.2) and dropping its first term because it is not a function of τ_m and f_m^d, we get (3.26). Also if SC has uncorrelated Gaussian disturbance with power $\sigma_v^2 = 1$ (i.e., $\mathbf{\Sigma}_v = \mathbf{I}_N$) then we have from section 3.1 $\mathbf{\Sigma}_v^m = \beta_m \mathbf{I}_N$ and if we use it, we can simplify (3.26) to (3.27).

Vita

Mohammed Rashid was born in Ames, Iowa in 1990. He received the B.Sc. degree in electrical engineering from NWFP University of Engineering and Technology, Pakistan, in 2012. He is the recipient of University Gold Medal for outstanding performance in that degree program. Currently, he is a Graduate Research and Teaching Assistant in the division of electrical and computer engineering at Louisiana State University, USA.

His research interest is in the areas of statistical signal processing, optimizing algorithms, machine learning, and passive radar.